Evolution of Differential Invariant Signatures and Applications to Shape Recognition

A DISSERTATION
SUBMITTED TO THE FACULTY OF THE GRADUATE SCHOOL
OF THE UNIVERSITY OF MINNESOTA
BY

Joseph Patrick Kenney

IN PARTIAL FULFILLMENT OF THE REQUIREMENTS
FOR THE DEGREE OF
Doctor Of Philosophy

August, 2009

Acknowledgements

I would like to thank my loving family, especially my father, I wish you could see this. I would also like to thank Peter Olver for providing good ideas and letting me run with them, and telling me when I might have run too far, and to the math department of the University of Minnesota.

Contents

List of Figures

Chapter 1

Introduction

Differential invariants are widely used in image processing and differential invariant signatures have been suggested as a way of recognizing shapes by Olver et.al.[12]. Although differential invariant signatures classify a curve up to a group motion, it is not obvious how to compare two different signatures. On top of this differential invariants are not very stable under noise. For example, consider two curves, one of which is a small perturbation of the first curve. These two curves would be close in Hausdorff distance, but the differential invariants on these two curves would most likely be wildly different. We would like to show that problems with noise can be overcome by smoothing the data and that differential invariants can be used to compare and classify curves.

The curve shortening flow, studied by Gage, Hamilton[24], Grayson, [26], Angenent [3],[4] and many others, also known as the geometric heat equation, empirically smoothes curves. It is the flow which most rapidly decreases the arc length of the curve. These flows have also been widely used in image processing [13],[47],[9] and has been suggested as a tool in shape modeling [34], and gives rise to the the curvature scale space [40],[39],[41]. It has also been modified to use in image segmentation by including a forcing or data-fidelity term to align the curve with boundaries found in an image [29]. Higher dimensional versions have also been suggested as a method for smoothing surfaces [48],[18].

Using the machinery of the invariant variational complex [31],[51], we can study the evolution of the differential invariant signature under these flows. By studying the evolution of the signature we can find special solutions and the evolution of certain geometric quantities related to these curve flows. Properties of the signature flow may also tell us about properties of the curve flow. Under the curve shortening flow the number of vertices, or local extrema of curvature, is non-increasing in time. This fact becomes apparent from the structure of the partial differential equation that the signature solves. The signature flow also lets us extend this result to different curve flows. While the curve shortening flow is invariant under Euclidean motions, we are not restricted to that group. The methods found in [51] are also valid for other transformation groups. We provide three more examples, the equi-affine and similarity group acting on planar curves and the centro-affine group acting on space curves. We provide a short analysis of the partial differential equations that arise from curve flows that are invariant under these actions.

After we look at a number of signature flows, we turn our attention to applying invariant signatures. The goal is to find a way of comparing two shapes. For a general overview of the field we refer the reader to the survey [33]. First we needed to create a labeled dataset of curves. Each curve with the same label should represent roughly the same shape or object. For example, if we have a number of different curves that all represent the outline of a particular wolf in a particular pose, then all of these curves would have the same label. We start with the Berkeley Segmentation Dataset [35] which consists of 300 images, each hand segmented by 10 to 15 different subjects. The boundary of each segmented region gives a curve. After some processing and discarding a large number of the images we are left with 350 curves with 33 different labels. Each label has at least five different curves. These curves differ in two main ways: occlusion, and the amount of detail provided. While differential invariant signatures are local and handle occlusions gracefully, they are not stable with regards to slight perturbations of the curve. We present a novel method for comparing two signatures. After smoothing

this set of curves we build a classifier that performs fairly well classifying the curves.

The new results in this thesis fall into two areas: a collection of results about various invariant planar curve flows obtained by studying the evolution of the signature function, and a study of a particular dataset showing that differential invariant signatures can be used to classify curves when the curves are appropriately smoothed.

Chapter 2

Foundations of differential invariants

We begin by discussing differential invariants, Cartan's method of normalization, the modern theory of regularized group actions, and signature manifolds and the invariantized variational complex. The theory goes back to the work done on moving frames by Cartan [14],[15], and later updated by Mark Fels and Peter Olver in [50],[22]. The final section of this chapter covers the machinery in [51] which allows us to compute the evolution of differential invariants under invariant submanifold flows.

2.1 Transformation groups and normalization

Here we define transformation groups and define some useful properties. We also describe the properties that we need to ensure that a moving frame exists. All of our algorithms require a moving frame to create invariants, so it is important to know when one can be constructed.

Definition A *transformation group* acting on a smooth manifold M is given by a Lie group G along with a smooth map $\Phi : G \times M \to M$, denoted by $\Phi(g, x) = g \cdot x$

which satisfies

$$e \cdot x = x, \quad g \cdot (h \cdot x) = (g \cdot h) \cdot x, \quad \text{for all} \quad x \in M, g \in G. \tag{2.1}$$

It follows from the definition that the transformation induced by the group element g^{-1} is the inverse transformation to that induced by g. Definition 2.1 assumes that the group action is defined globally, but at times it makes sense to only consider a local group action. At a point $x \in M$ the function Φ may be defined for only some subset of group elements sufficiently close to the identity e. A *local transformation group* is a function Φ defined on some open subset V, $\{e\} \times M \subset V \subset G \times M$ with the restriction (2.1) defined wherever it makes sense.

Example One example of a group acting on a manifold is Euclidean transformation group $G = SO(2) \ltimes \mathbb{R}^2$ acting on $\mathbb{R}^2$. The group elements can be represented by three parameters (a, b, θ) and the corresponding transformation is given by

$$g \cdot (x, y) = (x \cos\theta - y \sin\theta + a, x \sin\theta + y \cos\theta + b). \tag{2.2}$$

Given an action of a Lie group G on a manifold M, the *isotropy group* of a point $x \in M$ is the group of of elements which fix x, $G_x = \{g | g \cdot x = x\}$. A group acts *freely* on M if all of the isotropy groups are trivial, $G_x = \{e\}$ for all $x \in M$. The group acts *locally freely* if this holds for all group elements that are sufficiently close to the identity, $G_x \cap N_e = \{e\}$ for all $x \in M$, where N_e is some neighborhood of the identity. This is equivalent to the isotropy subgroups being discrete subgroups of G. A group action is *effective* if $g \cdot x = h \cdot x$ for all $x \in M$ if and only if $g = h$. In other words the only element which acts as the identity is the identity. The *global isotropy group* is the intersection over the manifold M of all isotropy groups, $G_M = \cap_{x \in M} G_x$. The action of G is effective if and only if $G_M = \{e\}$. A group action is called *locally effective* if G_M is a discrete subset of G. Any free group action is necessarily effective. A group action is *effective on subsets* if for every open subset $U \subset M$ the isotropy group $G_U = e$. A group

action is said to be *locally effective on subsets* if the isotropy group G_U is discrete for every open subset $U \subset M$.

If a group action is not effective we can replace it with an effective action by taking the quotient with the global isotropy group.

Proposition 2.1 *Suppose G is a Lie group acting on a manifold M with a global isotropy group G_M. The group G_M is a normal Lie subgroup of G, and the action of the group G/G_M is a well-defined, effective action on M which coincides with the action of G. This means that if g and $\tilde{g}$ have the same action on M then there is an element $h \in G_M$ such that $\tilde{g} = g \cdot h$, so $\tilde{g}, g$ are representatives of the same coset in G/G_M.*

For the rest of this paper we assume all groups act effectively unless otherwise noted.

Given a transformation group G acting on a manifold M a subset $S \subset M$ is called G-invariant if it is left unchanged under the action of G. In other words, if $x \in S$ then $g \cdot x \in S$ for all $g \in G$. If we are working with a local transformation group then this restriction only needs to hold for $g \in G$ for which $g \cdot x$ is defined. Varieties, the zero set of a given set of equations

$$S_F = \{x | F_1(x) = ... = F_p(x) = 0\}, \tag{2.3}$$

are important in the study of differential equations. A group G is called a *symmetry group* of the system of equations $F_1(x) = ... = F_p(x) = 0$ if S_F is G-invariant. If we have a solution x to the equations $F(x) = 0$ and a symmetry group G, then $g \cdot x$ is also a solution for all $g \in G$. A function defined on M may also be invariant under a group action.

Definition A function $F : M \to \mathbb{R}$ is invariant under the group action G if

$$F(z) = F(g \cdot z) \quad \forall g \in G.$$

A connected Lie transformation group G is generated by a set of vector fields on M named the *infinitesimal generators*. The infinitesimal generators tell us exactly which functions are invariant under a group action.

Theorem 2.2 *Let G be a connected transformation group acting on a manifold M. A function $F : M \to \mathbb{R}$ is invariant under G if and only if*

$$\mathbf{v}[F] = 0$$

for all $x \in M$ and every infinitesimal generator $\mathbf{v}$ of G.

We can use this condition to find differential invariants, but it amounts to solving a system of differential equations.

The *orbit* of a transformation group is the image of a point under all the group transformations $\mathcal{O}_x = \{g \cdot x | g \in G\}$. Orbits are the minimal nonempty invariant subsets. If the group action is free then the orbits will themselves be submanifolds of the manifold M.

Definition The group action is *semi-regular* if all of its orbits have the same dimension.

Definition The group action is *regular* if it is semi-regular and at each point $z \in M$ there is an arbitrarily small neighborhood, such that the intersection of the neighborhood and any orbit is a connected set.

The regularity condition eliminates some pathological cases, such as the irrational flow on the torus. The orbits of the irrational flow are one-dimensional, but they are also dense in the two-dimensional torus. The regularity of the group action is also essential in building the moving frame so we assume that all of the group actions for the rest of the thesis are regular.

Proposition 2.3 *An r-dimensional Lie group G acts effectively freely on a manifold M if and only if its orbits have the same dimension r as G itself.*

The orbits of regular group actions can be given simple local coordinates.

Theorem 2.4 *Let G be a Lie group acting regularly on a manifold M with r-dimensional orbits. We can find rectifying local coordinates near every point on*

the manifold M, $(y, z) = (y^1, ..., y^r, z^1, ..., z^{m-r})$, such that any orbit intersects the coordinate chart in at most one slice $N_c = \{z^1 = c_1, ..., z^{m-r} = c_{m-r}\}$, at every point for constants $c = (c_1, ..., c_{m-r})$.

The existence of these coordinates is a result of Frobenius' theorem, which states that the orbits form a foliation of the manifold M. The y coordinates can be seen as group parameters and the z coordinates form a set of functionally independent invariants under the group action.

Moving frames

We now look at moving frames. Many classical moving frames, such as the Darboux frame, or the Frenet-Serret frame, are an ordered set of smoothly varying vector fields defined at points of a submanifold $S \subset M$. The Darboux frame is defined at non-umbilical points on surfaces in $\mathbb{R}^3$. The Frenet-Serret frame is defined on curves in $\mathbb{R}^3$ at points where the torsion is non-zero. The modern approach is to define the moving frame as a particular map from the manifold to the transformation group. Unless otherwise noted, G is an r-dimensional Lie group acting smoothly on M, an m-dimensional manifold.

Definition A smooth map $\rho : M \to G$ is *left G-equivariant* if $\rho(g \cdot z) = g \cdot \rho(z)$ for all $g \in G, z \in M$. A smooth map $\rho : M \to G$ is *right G-equivariant* if $\rho(g \cdot z) = \rho(z) \cdot g^{-1}$ for all $g \in G, z \in M$. A (left, right) moving frame is a (left,right) G-equivariant map.

Most classical moving frames are left moving frames, and left and right moving frames are closely related. If $\rho(z)$ is a left moving frame, then its inverse $\rho(z)^{-1}$ is a right moving frame. For our purposes right moving frames will be easier to compute, so we will be working with right moving frames.

Theorem 2.5 *A moving frame exists in a neighborhood of a point $z \in M$ if and only if G acts regularly and freely on M.*

Normalization

We can explicitly find a moving frame by using Cartan's method of normalization. The construction of the moving frame depends on a cross-section to the group orbits.

Definition Two submanifolds S, K of a manifold M intersect *transversally* if $TM_z = TS_z \oplus TK_z$ for all $z \in S \cap K$.

Definition A *cross-section* to an orbit is a submanifold K which intersects the orbit transversally and at most once.

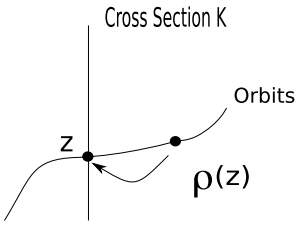

Figure 2.1: A cross section to the orbits of G

Theorem 2.6 *Let G act freely and regularly on M, and let K be a cross-section. Given $z \in M$, let $g = \rho(z)$ be the unique group element that maps z to the cross-section: $g \cdot z \in K$. Then $\rho : M \to G$ is a right moving frame for the group action.*

Given local coordinates $z = (z_1, ..., z_m)$ on M, let $w(g, z) = g \cdot z$ be the formulae for the transformed coordinates under the group transformation. The right moving frame $g = \rho(z)$ associated to the coordinate cross-section $K = \{z_1 = c_1, ..., z_r = c_r\}$ is found by solving the equations

$$w_1(g, z) = c_1, \quad ... \quad w_r(g, z) = c_r, \tag{2.4}$$

for the group parameters $(g_1, ..., g_r)$ in terms of the coordinates $z = (z_1, ..., z_m)$. The remaining coordinates are our non-constant invariants.

Theorem 2.7 *If $g = \rho(z)$ is the moving frame solution to the equations 2.4 then*

$$I_1(z) = w_{r+1}(\rho(z) \cdot z), \quad \ldots \quad I_{m-r}(z) = w_m(\rho(z) \cdot z), \tag{2.5}$$

form a complete system of functionally independent invariants.

Any function on the manifold M can be invariantized using this method.

Definition The *invariantization* of a scalar function $F : M \to \mathbb{R}$ with respect to a right moving frame is the invariant function $I = \iota(F)$ defined by $I(z) = F(\rho(z) \cdot z)$.

On each orbit we set the function to be a constant, which is determined by the the function value at the cross-section. In particular the invariantization of an invariant function is itself, $I = \iota(I)$. The process of invariantization is a projection from functions to invariants.

2.2 Jet space

When a group G acts on a manifold M the action is often not free. Consider the case of the Euclidean group acting on $\mathbb{R}^2$. The Euclidean group is three-dimensional and $\mathbb{R}^2$ is only two dimensional, so the orbits cannot possibly be of the same dimension as the transformation group. Each point has a one parameter isotropy group, namely the rotations around that point. The group action must be extended to a manifold of higher dimension if we are to have any hope of it being free.

We recall that the Euclidean curvature is given by $\kappa = u_{xx}/(1+u_x^2)^{3/2}$, which is an invariant under the Euclidean group acting on curves in $\mathbb{R}^2$. We also note that it depends on derivatives, so we call it a *differential invariant*. One way to represent derivatives is through the jet space, which was first defined by Ehresmann [19]. Here we include a brief discussion of the basic ideas of jet spaces. Many of the details of the basic constructions such as vector fields and differential forms can be found in [49] and details of the variational bicomplex are available in a technical report by Ian M. Anderson [2]. We will only discuss differential invariants which

arise through prolongation to the jet space. A group action can also be extended by applying it to multiple copies of the manifold M, leading to joint invariants [45], or to multiple copies of the jet space. These methods are important to invariantizing numerical schemes and for calculating differential invariants on a discrete set of points.

Definition Given a smooth manifold M of dimension m and an integer $p < m$, the *k-th order jet bundle* $J^k = J^k(M, p)$ is a fiber bundle over M, such that the fiber of a point $z \in M$ consists of the set of equivalence classes of p-dimensional submanifolds of M with *k-th* order contact at z.

There is a natural projection between two jet spaces of different orders $\pi_l^k : J^k \to J^l$ when $k > l$. The inverse limit of the projections π_k^{k+1} gives rise to the infinite jet space $J^\infty = J^\infty(M, p)$ along with projection maps $\pi_k^\infty : J^\infty \to J^k$. The space J^∞ is called the infinite jet bundle over M. For $l < k$ we identify functions and differential forms on J^l with functions and forms on J^k under the pull-back $(\pi_l^k)^*$. Smooth functions and forms on J^∞ are defined as the direct limit of the space of smooth functions and forms on J^k.

We give the manifold M the local coordinates $(x^1, ..., x^p, u^1, ..., u^q)$ in some neighborhood where the submanifold S can be represented as a graph $u = u(x)$. The coordinates on the jet space $J^k = J^k(M, p)$ are given by

$$z^{(k)} = (x^1, ..., x^p, u_J^\alpha), \quad 1 \leq \alpha \leq q, \quad \#J \leq k,$$

where

$$u_J^\alpha = \frac{\partial^{\#J} u^\alpha}{(\partial x^1)^{j_1} ... (\partial x^p)^{j_p}}, \quad J = (j_1, ..., j_p)\,.$$

We also use the notation J, i where the multi-index J, i is the multi-index (j_1,j_2, ... ,$j_i + 1$, ... ,j_p).

The k-jet of S, $j^k S$, is itself a p-dimensional submanifold of J^k. Any differential form that vanishes on all k-jets is a *contact form*. The collection of all contact forms form a differential ideal on J^∞ called the *contact ideal*. In a given

a coordinate system the canonical contact forms are

$$\theta^\alpha_J = du^\alpha_J - \sum_{i=1}^{p} u^\alpha_{J,i} dx^i, \quad \alpha = 1, ..., q, \quad |J| \geq 0.$$

These form a basis for the contact ideal. Although these particular contact forms depend on the coordinate system, the contact ideal is intrinsic. It does not depend on the local coordinates.

The cotangent bundle on J^∞ splits into two sub-bundles, a horizontal sub-bundle spanned by the differential forms $dx^1, ..., dx^p$ and the vertical sub-bundle which is the contact ideal. The splitting of the cotangent bundle splits the differential d on J^∞ into two components, a horizontal and a vertical derivative

$$d = d_H + d_V.$$

The horizontal differential is given by

$$d_H F = \sum_{i=1}^{p} (D_i F) dx^i,$$

where

$$D_i = \frac{\partial}{\partial x^i} + \sum_{\alpha=1}^{q} \sum_J u_{J,i} \frac{\partial}{\partial u^\alpha_J}.$$

The total derivatives D_i span the subspace of total vector fields in the tangent bundle TJ^∞. The space which they span can also be defined as the set of vector fields that are annihilated by all forms in the contact ideal. This gives an intrinsic definition of this space since the contact ideal is intrinsic.

The vertical differential is defined by

$$d_V F = \sum_{\alpha=1}^{q} \sum_J \frac{\partial F}{\partial u^\alpha_J} d\theta^\alpha_J.$$

The vector fields $\frac{\partial}{\partial u^\alpha_J}$ span the subspace of vertical vector fields in TJ^∞. These vector fields can also be classified as those vector fields that are annihilated by the horizontal differential forms.

The splitting of the differential forms on J^∞ into horizontal and vertical components induces a bi-grading on the differential forms. Let $\mathbf{\Omega}^{r,s}$ be the set of differential forms which are the wedge product of r horizontal forms and s vertical forms. The horizontal differential d_H is a map from $\mathbf{\Omega}^{r,s}$ to $\mathbf{\Omega}^{r+1,s}$ and the vertical differential d_V is a map from $\mathbf{\Omega}^{r,s}$ to $\mathbf{\Omega}^{r,s+1}$. This splitting gives us the variational bicomplex.

Given a vector field on a manifold we need to know how this vector field is prolonged to the jet space. The k-th prolongation of the vector field

$$X = \sum_{i=1}^{p} \xi^i(x,u)\frac{\partial}{\partial x^i} + \sum_{\alpha=1}^{q} \varphi^\alpha(x,u)\frac{\partial}{\partial u^\alpha}$$

is defined as $pr^k X = (\pi_k^\infty)_* prX$. The k-th prolongation in terms of local coordinates is given as

$$pr^k X = \sum_{i=1}^{p} \xi^i(x,u)\frac{\partial}{\partial x^i} + \sum_{\alpha=1}^{1}\sum_{|J|\leq k} \varphi_J^\alpha(x,u^{(|J|)})\frac{\partial}{\partial u_J^\alpha}. \tag{2.6}$$

The functions $\varphi_J^\alpha(x,u)$ are given as

$$\varphi_J^\alpha(x,u) = D_J Q^\alpha + \sum_{i=1}^{p} \xi^i(x,u) u_{J,i}^\alpha, \tag{2.7}$$

where

$$Q^\alpha(x,u^{(1)}) = \varphi^\alpha(x,u) - \sum_{i=1}^{p} \xi^i(x,u) u_i^\alpha \tag{2.8}$$

are the components of the characteristic vector field X.

A connected transformation group G can be prescribed by its infinitesimal generators. Let the vector fields $\mathbf{v}_1, ..., \mathbf{v}_r$ be the prolongations of a basis for the infinitesimal generators of our transformation group. Since we are only considering curves, $p = 1$, in this thesis the vector fields can be written as

$$\mathbf{v}_\kappa = \xi_\kappa(x,u)\frac{\partial}{\partial x} + \sum_{\alpha=1}^{q}\sum_{j=0}^{n} \varphi_{J_\kappa}^\alpha(x,u)\frac{\partial}{\partial u_J^\alpha}. \tag{2.9}$$

The coefficients

$$\varphi^{\alpha}_{J,\kappa} = \mathbf{v}_{\kappa}(u^{\alpha}_{J})$$

are found using the recursion formula (2.7).

Definition The k-th order prolongation of a smooth transformation $g \in G$ on a manifold M is defined as

$$g^{(k)} \cdot j^k S = j^k (g \cdot S)$$

for any submanifold $S \subset M$.

We will often drop the superscript (k) and write the prolonged group element as g when the order of the prolongation is obvious from the context.

Definition A k-th order differential invariant is a locally defined function on $J^k(M, p)$ which is invariant under the k-th prolongation of the group action.

If $l < k$ any l-th order differential invariant is trivially a k-th order differential invariant under the map $(\pi^k_l)^*$.

Group orbits in lower order jet spaces are projections of group orbits from higher order jet spaces, so the dimension of the orbits can not decrease as the order of the jet space increases. The dimension of the orbits are also bounded by the dimension of the transformation group. Due to the pseudo-stabilization theorem, Theorem 5.37 in [49], the dimension of the orbits must stabilize at some order $n \leq r$. We call this n the *order of stabilization*. We denote $\mathcal{V}^n \subset J^n$ as the open set of points where the orbits obtain their maximum dimension. We call a point $z^{(k)} \in J^k$ a regular jet if $\pi^k_n \in \mathcal{V}^n$. If $z^{(k)}$ is a regular jet then the orbit $\mathcal{O}(z^{(k)})$ has maximum dimension. We denote the union of all regular jets as $\mathcal{V} \subset J^{\infty}$.

The following result, due to Ovsiannikov and Olver [52],[46], is necessary for the moving frames construction.

Theorem 2.8 *If the action of G on M is locally effective on subsets then the prolonged action is locally free on $\mathcal{V}^k$ for $k \geq n$ where n is the order of stabilization and $n \leq r = dim(G)$.*

The original form of this theorem, presented by Ovsiannikov, omitted the assumption that the action of G was locally effective on subsets, and only required the action to be locally effective. This assumption is not sufficient, as pointed out by Olver, who gives examples of totally singular jets in [46]. It seems likely that a global version of this theorem should hold, at least if the group action is analytic, but no such result is known.

The dimension of the orbits stabilizes at order n, so by Frobenius' theorem the nontrivial differential invariants appear at order $n+1$, if not earlier. However new differential invariants appear at each new order of prolongation, and there are an infinite number of them since we can continue the process of prolongation indefinitely. Fortunately this infinite set of differential invariants can be also produced by a generating set of invariants along with a set of invariant differential operators. The invariant differential operators are the dual vector fields to the horizontal contact invariant forms.

Definition A one-form ω on J^∞ is called a *contact invariant* form if it has the following property: For all $g \in G$ there exists a contact form θ_g such that $(g^{(n)})^*\omega = \omega + \theta_g$. A set of p linearly independent horizontal contact invariant forms $\{\omega^1, ..., \omega^p\}$ is called a *horizontal contact invariant coframe.*

A contact invariant coframe on $\mathcal{V}^n$ exists by previous results by Ovsiannikov [52] and Fels and Olver [21]. We will denote this coframe as $\{\omega^1, ..., \omega^p\}$. The horizontal differential of a function can be rewritten in terms of the particular contact invariant coframe as

$$d_H F = \sum_{i=1}^{p} (\mathcal{D}_i F)\, \omega^i.$$

The differential operators $\mathcal{D}_i$ are invariant differential operators. All of the differential invariants can be produced from the invariants appearing at order $n+1$ and their invariant derivatives.

Theorem 2.9 *Suppose G is a transformation group with order of stabilization n. In a neighborhood of a regular jet $z^{(n)} \in \mathcal{V}^{(n)}$ there exists a contact invariant coframe $\omega^1, ..., \omega^p$ and corresponding invariant differential operators $\mathcal{D}_1, ..., \mathcal{D}_p$. Moreover, there exists a generating set of differential invariants $\mathcal{I}_1, ..., \mathcal{I}_l$ of order at most $n+1$ such that any other invariant can be locally written as a function of the generating invariants and their derivatives*

$$I = H(I_1, ..., I_l, ..., \mathcal{D}_J I_j, ...),$$

where $\mathcal{D}_J$ is a composition of the invariant differential operators.

Differential invariants are found by applying the normalization process to the jet bundle of a manifold. An n^{th} order moving frame $\rho : J^n \to G$ is an equivariant map defined on an open subset of J^n.

The local coordinates in jet space will be denoted as $z^{(n)} = (x, u^{(n)})$. We denote the transformed local coordinates as $w = (y, v) = g \cdot (x, u)$. We will use the notation $w^{(n)} = (y, v^{(n)})$ to refer to the transformed local coordinates in jet space. The prolonged action on jet space can be found by implicitly differentiating v with respect to y.

Example Let us calculate one example. Suppose we have a curve $(x(t), u(t))$ with the restrictions $x'(t) \neq 0$, $u'(t) \neq 0, x(t) > 0, u(t) > 0$ and a transformation group given by

$$y = \alpha x, \qquad v = u^\beta.$$

Our transformation group has two dimensions. The jet space J^1 has three dimensions. Two of the local coordinates will be normalized to constants to solve for the group parameters (α, β). The transformed third coordinate will be our first non-constant differential invariant.

By prolongation we obtain

$$\frac{dv}{dy} = \frac{\beta u^{\beta-1} u_t}{\alpha x_t}.$$

We set $y = 1, v = e$, and solve the normalization equations for α, β

$$\alpha = x^{-1}, \qquad \beta = \frac{1}{\ln u}.$$

Then we substitute these values into $\frac{dv}{dy}$

$$\frac{dv}{dy} = \frac{x\, u^{(1/\ln u)-1}\, u_t}{\ln u\, x_t} = \frac{x u^{(1 \ln u)-1}}{\ln u}\, \frac{du}{dx}$$

which is the first differential invariant of this group action.

We can also find an invariant differential operator. We first find a contact invariant one-form. The invariant horizontal one-form dy is

$$dy = P dt = \alpha\, x_t\, dt = \frac{x_t}{x}\, dt.$$

The invariant differential operator related to this one-form is

$$\frac{d}{dy} = \frac{1}{P}\frac{d}{dt} = \frac{x}{x_t} D_t.$$

2.3 Equivalence and signature curves

All of the essential differential invariants can be produced by a certain generating set of invariants and a collection of invariant differential operators. These tell us about the local geometry of a curve, but we would also like to use the differential invariants to ask about the global equivalence of two curves, and symmetries of the curve.

Definition Let G be a transformation group acting on a manifold M. Two curves $C, \bar{C}$ or M are said to be *equivalent* if there is a group element $g \in G$ such that $C = g \cdot \bar{C}$. A symmetry of C is any group element $g \in G$ for which $C = g \cdot C$.

The equivalence and symmetry problem can be solved using the signature curve. Let n be the order of stabilization of the group action. Let $\{I_1, ..., I_{N_k}\}$ be a complete list of differential invariants for any $k \geq n$. In other words, any other

differential invariant of order k is a function of $\{I_1, ..., I_{N_k}\}$. Let $\tilde{I}_\alpha = I_\alpha|_{J^k S}$ be the restriction of the invariants to $j^k S$ and define $\phi^k : S \to \{\tilde{I}_1, ..., \tilde{I}_{N_k}\}$. Let $t_k = rank(\phi)$. Since $dim(S) = 1$ then t_k is either 0 or 1. We call the smallest value $s \geq n$ for which $t_s = t_{s+1}$, the *differential invariant rank* of the curve.

Definition A submanifold S is called regular if $j^n(S) \in \mathcal{V}^n$ and t_k does not vary on S for each $k \geq n$.

Definition The k^{th} order signature curve $\mathcal{C}^k$ of the submanifold S is the immersed manifold $Im(\phi^k) \subset \mathbb{R}^{N_k}$.

The differential invariant rank t_k is non-decreasing with respect to k since more differential invariants are included in the signature. Since it is at most 1 there are only a few possibilities to consider. The only possibilities for a regular curve are

$$t_n = 0, t_{n+1} = 0$$

$$t_n = 0, t_{n+1} = 1, t_{n+2} = 1, ...,$$

$$t_n = 1, t_{n+1} = 1, t_{n+1} = 1, ... \quad .$$

A complete set of generating differential invariants appears at order $n + 1$ by Theorem 2.9. In the first case all of these generating differential invariants are constant on the curve. Since they are constant, all of their derivatives, which are the higher order differential invariants, are 0. The rank of the signature of any order is 0. The curve can be classified by the values of the differential invariants.

We see an example of the second case when we look at the Euclidean group acting on planar curves. The group action stabilizes at $n = 1$. Since there are no non-constant first order differential invariants $t_n = 0$. If we have a regular curve that is not a line or a circle then the curvature is non-constant and $t_{n+1} = 1$. The final case occurs when non-constant differential invariants appear at the order of stabilization. This happens when we look at the centro-affine group acting on generic curves in $\mathbb{R}^3$, as we see in section 2.4.6. In the first and third case the differential invariant rank is $s = n$, and in the second case it is $s = n + 1$.

Theorem 2.10 *Let $C, \bar{C}$ be analytic, regular one-dimensional submanifolds of M. The submanifolds $C, \bar{C}$ are equivalent if and only if they have the same differential invariant order s and $\mathcal{C}^{s+1}(S) = \mathcal{C}^{s+1}(\bar{S})$.*

The signature is a system of ordinary differential equations for the functions $u^\alpha(x)$. Given initial values for $u^\alpha, u^\alpha_j, j < s$, the system has a unique local solution. The entire curve can be found by analytic continuation.

Example In the case of the Euclidean group acting on planar curves we see that the order of stabilization is $n = 1$. There are no independent differential invariants at order one; at order two there is one independent differential invariant κ. At a generic point $rank(\phi^2) = 1 = p$ so the differential invariant order is $s = 2$. A regular planar curve is characterized by its signature $\mathcal{C}^3(S) = \{(\kappa(z), \kappa_s(z) | z \in S\}$.

Signatures also tell us when a submanifold is self-similar.

Theorem 2.11 *A submanifold S of differential invariant rank t has a $(p-t)$-dimensional isotropy group G_S acting locally freely on the submanifold S.*

Example We again consider the 3-dimensional Euclidean group acting on planar curves. The 0-dimensional signatures that correspond to 1-dimensional submanifolds are the points $(\kappa, 0)$. The corresponding submanifolds are lines, when $\kappa = 0$, and circles when κ is a non-zero constant. Lines have a one-dimensional symmetry group, namely translations along the direction vector, and circles also have a one-dimensional symmetry group, rotations about the center of the circle.

If a submanifold has full differential invariant rank $t = p$ then its isotropy group is discrete. If the index of a generic point on the signature curve is equal to one, then there are no other points on the original curve that match it and the symmetry group will only consist of the identity. Consider a non-circular ellipse, under the proper Euclidean group. Its symmetry group consists of 2 elements, the identity and a rotation by π. The differential invariants κ, κ_s will be equal at opposite points of the ellipse, so the index of the signature will be 2. In general,

for regular curves, the number of elements in the symmetry group will be equal to the index of a generic point on the signature,

$$|G_S| = |\phi^{-1}(c)|.$$

While the signature classifies a regular curve up to motion by a group action, the regularity condition is important as pointed out by Nicoldi et.al. [43]. Suppose we have a portion of the curve where the curvature is constant. At these points the invariant rank drops to 0 and the signature that corresponds to these segments is just a point $(\kappa, 0)$. The signature does not contain any information on the arc length of these circular arcs. These sections of the curve can be replaced with a circular segment of the same curvature and any length, and it will not change the signature. Unless the curve is fully a circle it is not regular as the differential invariant rank is not constant on the curve. The only information that is missing on these arcs is the arc length, so the signature curve could be extended to include a weighting at these points that would indicate the length of the arc of constant curvature. This issue can also be avoided by only working with analytic curves. If we restrict ourselves to analytic curves. In the above example we would have a portion of the curve where $\kappa_s = \kappa_{ss} = \kappa_{sss} = ... = 0$. By analytic continuation the curvature would be constant on the entire curve.

2.4 Invariant variational complex

2.4.1 Regularized group actions

We have described the basics of the variational bicomplex and differential invariants. In this section we discuss a modern version Cartan's method of moving frames due to Olver and Kogan [31] which leads to the invariant variational complex. Now we are ready to describe how the invariantization process applies to the variational bicomplex. We follow the regularization procedure presented in [22]. For a given group action G on a manifold M, we consider the the lifted action

$g \cdot (h, z) = (h \cdot g^{-1}, g \cdot z)$ of G on the right principal bundle $\sigma : \mathcal{B} = G \times M \to M$. This group action is always free and regular on $\mathcal{B}$. A complete set of functionally independent lifted invariants on $\mathcal{B}$ are provided by the evaluation map $\tau : \mathcal{B} \to M$, defined by $\tau(g, z) = g \cdot z$.

This construction can be applied to the prolonged action $G^{(n)}$ on J^n. In the infinite limit we have the regularized jet bundle $\sigma : \mathcal{B}^\infty = G \times J^\infty \to J^\infty$ given by $\sigma(g, z^{(\infty)}) = z^{(\infty)}$, along with the lifted group action

$$g \cdot (h, z^{(\infty)}) = \left(h \cdot g^{-1}, g^{(\infty)} \cdot z^{(\infty)}\right), \quad g \in G, \quad (h, z^{(\infty)}) \in \mathcal{B}^\infty.$$

The components of the evaluation map,

$$\tau(g, z^{(\infty)}) = g^{(\infty)} \cdot z^{(\infty)},$$

give a complete set of differential invariants on $\mathcal{B}$. This gives the lifted jet space a double filtration or groupoid structure.

A moving frame on the infinite jet bundle, $\rho : J^\infty \to G$, defines a G-equivariant section $\tilde{\sigma} : J^\infty \to \mathcal{B}^\infty$, specifically $\tilde{\sigma}(z^{(\infty)}) = (\rho(z^{(\infty)}), z^{(\infty)})$. The map $\tau \cdot \tilde{\sigma} : J^\infty \to J^\infty$ is given by

$$\rho(z^{(\infty)}) \cdot z^{(\infty)}.$$

The components of this map define the fundamental normalized differential invariants. For any differential function $F : J^\infty \to \mathbb{R}$, we define its *lift* as $\hat{F}(g, z^{(\infty)}) = \tau^* F$, which is an invariant function on $\mathcal{B}^\infty$. We define the *invariantization* of F as $\iota(F) = \tilde{\sigma}^* \hat{F}$. The invariantization of a function is the unique differential function that agrees with F on the cross-section we used to define our moving frame. Invariantization is a projection from differential functions to differential invariants, so if a function is already invariant, then it is equal to its invariantization.

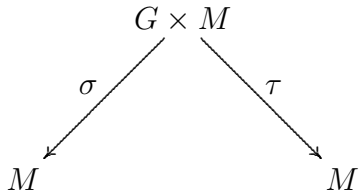

We denote the space of *lifted differential forms* on $\mathcal{B}^\infty$ as $\hat{\mathbf{\Omega}}^*$. A *coframe*, or basis, for $\hat{\mathbf{\Omega}}^*$ can be broken down into three parts, the pulled back horizontal forms dx^i, $i = 1...p$, the contact one-forms θ^α_J, $\alpha = 1...q$, $\#J \geq 0$ and the Maurer-Cartan forms μ^j, $j = 1...r$ on G. We denote $\hat{\mathbf{\Omega}}^{j,k}$ as the space of forms with j jet components, the horizontal or contact forms, and k group components, the Maurer-Cartan forms. The differential breaks into a jet component and a group component

$$d = d_J + d_G$$

with

$$d_J : \hat{\mathbf{\Omega}}^{j,k} \to \hat{\mathbf{\Omega}}^{j+1,k}, \quad d_G : \hat{\mathbf{\Omega}}^{j,k} \to \hat{\mathbf{\Omega}}^{j,k+1}.$$

This decomposition gives a trivial bicomplex structure on $\mathcal{B}^\infty$

$$d_J^2 = 0, \quad d_J d_G + d_G d_J = 0, \quad d_G^2 = 0.$$

We denote the space $\hat{\mathbf{\Omega}}_J = \oplus_j \hat{\mathbf{\Omega}}^{j,0}$ as the space of pure jet forms. The *jet projection* $\pi_J : \hat{\mathbf{\Omega}}^* \to \hat{\mathbf{\Omega}}_J$ eliminates the Maurer-Cartan forms. Although the coefficients of the Maurer-Cartan forms are now 0, the coefficients of the jet forms may still depend on the group parameters. Its interactions with the differential are

$$\pi_J \cdot d = d_J = d_J \circ \pi_J, \quad \pi_J \circ d_G = 0, \quad \text{but} \quad d_G \circ \pi_J \neq 0.$$

If Ω is a differential form on J^∞, then $\hat{\Omega} = \pi_J \tau^* \Omega$ is the corresponding *lifted jet form* on $\mathcal{B}^\infty$. This can also be realized as the pull back of Ω under the prolonged group transformation

$$\hat{\Omega}|_{(g,z^{(\infty)})} = \pi_J \tau^* (\Omega|_{z^{(\infty)}}) = g^* (\Omega|_{g^{(\infty)} \cdot z^{(\infty)}}),$$

which we instead write as $\hat{\Omega} = g^* \Omega$. Since G acts on $\mathcal{B}^\infty$ by the product action the forms $\tau^* \Omega$ and $\hat{\Omega} = \pi_J \tau^* \Omega$ are both G-invariant, $g^* \hat{\Omega} = \hat{\Omega}$, for all $g \in G$. In local coordinates we have the *lifted horizontal forms*

$$d_J y^i = \pi_J (dy^i) = \pi_J \tau^* (dx^i), \quad i = 1...p$$

and the *lifted contact forms*

$$\Theta^\alpha_J = \pi_J \tau^*(\theta^\alpha_J) = \pi_J(dv^\alpha_J - \sum_{i=1}^p v^\alpha_{J,i} dy^i)$$
$$= d_J v^\alpha_J - \sum_{i=1}^p v^\alpha_{J,i} d_J y^i = d_V v^\alpha_J - \sum_{i=1}^p v^\alpha_{J,i} d_V y^i$$

Now we use the moving frame section $\tilde{\sigma} : J^\infty \to \mathcal{B}^\infty$ to pull back the lifted jet forms to invariant differential forms on J^∞.

Definition The *invariantization* of a differential form Ω on J^∞ is the differential form

$$\iota(\Omega) = \tilde{\sigma}^*(\pi_J(\tau^*\Omega)).$$

Given the local coordinates $z^{(\infty)} = (x, u^{(\infty)})$ the *invariant horizontal one-forms* are

$$\varpi^i = \tilde{\sigma}^*(d_J y^i) = \iota(dx^i).$$

These forms are not necessarily purely horizontal forms. If we decompose them into horizontal and contact forms,

$$\varpi^i = \omega^i + \eta^i, \quad \omega^i = \tilde{\sigma}^*(D_H y^i), \quad \eta^i = \tilde{\sigma}^*(d_V y^i),$$

the horizontal components $\omega^i = \pi_H(\varpi^i) = \tilde{\sigma}^*(d_H y^i) \in \Omega^{1,0}$ are the usual contact invariant horizontal one-forms. There are also correction terms $\eta^i \in \Omega^{0,1}$ that are needed to make the forms fully invariant. The fundamental invariant contact forms are given by

$$\vartheta^\alpha_J = \tilde{\sigma}^*(\Theta^\alpha_J) = \iota(\theta^\alpha_J).$$

These are true contact forms and they form a basis for the contact ideal. Invariantization is an exterior algebra morphism, so it is fully determined by its action on the coordinates, the horizontal one-forms dx^i and the contact forms θ^α_J. The corresponding dual invariant total derivatives are defined so that

$$d_{\mathcal{H}} F = \sum_{i=1}^p (\mathcal{D}_i F)\varpi^i, \quad d_{\mathcal{H}}\Omega = \sum_{i=1}^p \varpi^i \wedge (\mathcal{D}_i \Omega) \tag{2.10}$$

for any differential function F or differential form Ω. The invariant vertical derivative of a function is defined as

$$d_{\mathcal{V}} F = \sum_{\alpha, J} \frac{\partial F}{\partial u^\alpha_J} \vartheta^\alpha_J. \tag{2.11}$$

Example Euclidean geometry of planar curves

Consider the action

$$y = g^*(x) = x\cos\phi - u\sin\phi + a, \quad v = g^*(u) = x\sin\phi + u\cos\phi + b \tag{2.12}$$

of the 3 dimensional planar Euclidean group $SE(2)$ acting on plane curves $C \subset \mathbb{R}^2$. For convenience we assume that locally our curve is given as the graph of a function $u = f(x)$. Extending the following procedure to parameterized curves leads to more complicated formulae for the invariants, but the interrelationships are the same.

The prolonged group transformations

$$\begin{aligned}
v_y &= g^*(u_x) = \frac{\sin\phi + u_x\cos\phi}{\cos\phi - u_x\sin\phi} \\
v_{yy} &= g^*(u_{xx}) = \frac{u_{xx}}{(\sin\phi + u_x\cos\phi)^3} \\
v_{yyy} &= \frac{3\sin\phi u_{xx}^2 + (\cos\phi - \sin\phi u_x)u_{xxx}}{(\cos\phi - \sin\phi u_x)^5} \\
v_{yyyy} &= \frac{15u_{xx}^3\sin^2\phi - 10\sin\phi\,(u_x\sin\phi - \cos\phi)\,u_{xxx}\,u_{xx} + (\cos\phi - u_x\sin\phi)^2\,u_{xxxx}}{(\cos\phi - u_x\sin\phi)^7}
\end{aligned} \tag{2.13}$$

are found by implicit differentiation. Using the cross-section

$$K^1 = \{y = v = v_y = 0\} \subset J^1, \tag{2.14}$$

we solve the normalization equations $y = 0, v = 0, v_y = 0$ for the group parameters (ϕ, a, b) and find the local right-equivariant moving frame

$$\phi = -\tan^{-1} u_x, \quad a = -\frac{x + uu_x}{\sqrt{1 + u_x^2}}, \quad b = \frac{xu_x - u}{\sqrt{1 + u_x^2}}. \tag{2.15}$$

This is only a local moving frame due to the ambiguity in the rotation angle. The cross-section equations (2.14) still hold for $\tilde{\phi} = \phi + \pi$. Away from an inflection point we can fix this ambiguity by enforcing the condition $v_{yy} > 0$.

The fundamental differential invariants are then found by substituting the moving frame formulae (2.15) into (2.13) giving

$$\begin{aligned}
H &= \iota(x) = 0 \\
I_0 &= \iota(u) = 0 \\
I_1 &= \iota(u_x) = 0 \\
I_2 &= \iota(u_{xx}) = \kappa = \frac{u_{xx}}{(1+u_x^2)^{\frac{3}{2}}} \\
I_3 &= \iota(u_{xxx}) = \frac{u_{xxx}u_x^2 - 3u_{xx}^2 u_x + u_{xxx}}{(1+u_x^2)^3} = \kappa_s \\
I_4 &= \iota(u_{xxxx}) = \kappa_{ss} + 3\kappa^3
\end{aligned}$$

and so on. The invariants H, I_0, I_1 are the phantom invariants and $I_2 = \kappa$ is the Euclidean curvature. Contrary to expectations, we note that $I_4 \neq \kappa_{ss}$.

We can use the moving frame to find the invariantized version of the horizontal form.

$$\begin{aligned}
\varpi = dy = \cos\phi\, dx - \sin\phi\, du &= \frac{1}{\sqrt{1+u_x^2}}\, dx + \frac{u_x}{\sqrt{1+u_x^2}}\, du \\
&= \frac{1}{\sqrt{1+u_x^2}}\, dx + \frac{u_x}{\sqrt{1+u_x^2}}\, \theta + \frac{u_x^2}{\sqrt{1+u_x^2}}\, dx \\
&= \frac{1+u_x^2}{\sqrt{1+u_x^2}}\, dx + \frac{u_x}{\sqrt{1+u_x^2}}\, \theta \\
&= \sqrt{1+u_x^2}\, dx + \frac{u_x}{\sqrt{1+u_x^2}}\, \theta = ds + \eta
\end{aligned}$$

The invariantized horizontal form is a combination of the contact-invariant arc length form $\omega = ds$ and a contact correction term η. The dual invariant differential operator is

$$\mathcal{D} = D_s = (1+u_x^2)^{-1/2} D_x.$$

The invariant contact form can be found by pulling back $dv - v_y dy$ through our moving frame. Since we chose to normalize v_y as 0 we only need to pull back dv

$$dv = \sin\phi\, dx + \cos\phi\, du = \frac{-u_x}{\sqrt{1+u_x^2}}\, dx + \frac{1}{\sqrt{1+u_x^2}}\, du = \frac{\theta}{\sqrt{1+u_x^2}}.$$

2.4.2 Recurrence relations

In our example (2.4.1) we saw that $I_4 \neq \kappa_{ss}$, which is a hint that the invariantization process and differentiation do not commute. The following theorem tells us how to differentiate invariant differential forms.

Theorem 2.12 *If Ω is any differential form on J^n, then*

$$d\iota(\Omega) = \iota(d\Omega) + \sum_{\kappa=1}^{r} \nu^\kappa \wedge \iota[\mathbf{v}_\kappa(\Omega)] \tag{2.16}$$

where $\nu^1, ..., \nu^r$ are the invariantized Maurer-Cartan forms associated with the moving frame.

To take a closer look at each part of the formula (2.16), we rewrite the invariant Maurer-Cartan forms in terms of the invariant horizontal and contact forms

$$\nu^\kappa = \gamma^\kappa + \epsilon^\kappa, \quad \text{where} \quad \gamma^\kappa = R^\kappa \varpi, \quad \epsilon^\kappa = \sum_{\alpha,J} S_\alpha^{\kappa,J} \vartheta_J^\alpha. \tag{2.17}$$

The coefficients R^κ are known as the Maurer-Cartan invariants and $S_\alpha^{\kappa,J}$ are also differential invariants.

Now let's break up formula 2.16 into horizontal and vertical components. The Lie derivative does not preserve the bi-grading of our complex. The vector field $\mathbf{v}_\kappa$ preserves the contact ideal, but if $\mathbf{v}_\kappa(x) = \xi_\kappa(x,u)$, then $\mathbf{v}_\kappa(dx) = d\xi_\kappa = d_H\xi_\kappa + d_V\xi_\kappa$ which contains horizontal and zeroth order contact forms. If $\Omega \in \mathbf{\Omega}^{r,s}$ then $\mathbf{v}_\kappa(\Omega) \in \mathbf{\Omega}^{r,s} \oplus \mathbf{\Omega}^{r-1,s+1}$ and $d\Omega \in \mathbf{\Omega}^{r+1,s} \oplus \mathbf{\Omega}^{r,s+1}$. So, by formula (2.16), if $\tilde{\Omega} \in \tilde{\mathbf{\Omega}}^{r,s}$ then $d\tilde{\Omega} \in \tilde{\mathbf{\Omega}}^{r+1,s} \oplus \tilde{\mathbf{\Omega}}^{r,s+1} \oplus \tilde{\mathbf{\Omega}}^{r-1,s+2}$.

Using formulas (2.16) and (2.17) we can decompose the differential $d = d_{\mathcal{H}} + d_{\mathcal{V}} + d_{\mathcal{W}}$ into its component parts:

$$d_{\mathcal{H}}(\iota(\Omega)) = \iota(d_H\Omega) + \sum_{\kappa=1}^{r} \gamma^{\kappa} \wedge \iota(\pi_{r,s}(\mathbf{v}_{\kappa}(\Omega))),$$
$$d_{\mathcal{V}}(\iota(\Omega)) = \iota(d_V\Omega) + \sum_{\kappa=1}^{r} [\epsilon^{\kappa} \wedge \iota(\pi_{r,s}(\mathbf{v}_{\kappa}(\Omega))) + \gamma^{\kappa} \wedge \iota(\pi_{r-1,s+1}(\mathbf{v}_{\kappa}(\Omega)))]$$
$$d_{\mathcal{W}}(\iota(\Omega)) = \sum_{\kappa=1}^{r} \epsilon^{\kappa} \wedge \iota(\pi_{r-1,s+1}(\mathbf{v}_{\kappa}(\Omega))),$$

where

$$d_{\mathcal{H}} : \tilde{\mathbf{\Omega}}^{r,s} \to \tilde{\mathbf{\Omega}}^{r+1,s}, \qquad d_{\mathcal{V}} : \tilde{\mathbf{\Omega}}^{r,s} \to \tilde{\mathbf{\Omega}}^{r,s+1}, \qquad d_{\mathcal{W}} : \tilde{\mathbf{\Omega}}^{r,s} \to \tilde{\mathbf{\Omega}}^{r-1,s+2}.$$

Decomposing the formula $d^2 = 0$ we find

$$d_{\mathcal{H}}^2 = 0, \quad d_{\mathcal{H}}d_{\mathcal{V}} + d_{\mathcal{V}}d_{\mathcal{H}} = 0,$$
$$d_{\mathcal{W}}^2 = 0, \quad d_{\mathcal{V}}d_{\mathcal{W}} + d_{\mathcal{W}}d_{\mathcal{V}} = 0$$
$$d_{\mathcal{V}}^2 + d_{\mathcal{H}}d_{\mathcal{W}} + d_{\mathcal{W}}d_{\mathcal{H}} = 0$$

The invariantized Maurer-Cartan forms $\nu^1, ..., \nu^r$ can be found by pulling back the dual Maurer-Cartan forms $\mu^1, ..., \mu^r$ on G by the moving frame map $\nu^{\kappa} = \rho^*\mu^{\kappa}$. Fortunately, the invariantized Maurer-Cartan forms can also be found directly using the phantom differential invariants.

Lemma 2.13 *Let $I_1 = \iota(z_1), ...I_r = \iota(z_r)$ be the invariants related to the cross section coordinates $z_1, ..., z_r \subset (x, ...u_J^{\alpha}...)$ as defined in 2.4. Then*

$$0 = dI_{\varsigma} = d\iota(z_{\varsigma}) = \iota(dz_{\varsigma}) + \sum_{\kappa=1}^{r} \nu^{\kappa} \wedge \iota[\mathbf{v}_{\kappa}(z_{\varsigma})], \quad \varsigma = 1...r$$

can be solved uniquely for $\nu^1, ..., \nu^r$.

In particular we differentiate the fundamental differential invariants to find

$$dH = \varpi + \sum_{\kappa=1}^{r} \iota(\xi_{\kappa})\nu^{\kappa}, \quad dI_j^{\alpha} = I_J^{\alpha}\varpi^i + \varphi_J^{\alpha} + \sum_{\kappa=1}^{r} \iota(\varphi_{J_{\kappa}}^{\alpha})\nu^{\kappa}. \tag{2.18}$$

Putting together (2.17) and (2.10) we find the invariant derivatives

$$\mathcal{D}H = 1 + \sum_{\kappa=1}^{r} R^{\kappa}\iota(\xi_{\kappa}), \quad \mathcal{D}I^{\alpha}_{J+1} = I^{\alpha}_{Ji} + \sum_{\kappa=1}^{r} R^{\kappa}\iota(\varphi^{\alpha}_{J\kappa}). \tag{2.19}$$

The contact components in (2.18) yield

$$d_{\mathcal{V}}H = \sum_{\kappa=1}^{r} \iota(\xi_{\kappa})\epsilon^{\kappa}, \quad d_{\mathcal{V}}I^{\alpha}_{J} = \vartheta^{\alpha}_{J} + \sum_{k=1}^{r} \iota(\phi^{\alpha}_{J\kappa})\epsilon^{\kappa}. \tag{2.20}$$

Next we apply (2.16) to the invariantized horizontal differential forms.

$$d\varpi = \sum_{\kappa=1}^{r} \iota(D\xi_{\kappa})\nu^{\kappa} \wedge \varpi + \sum_{\kappa=1}^{r}\sum_{\alpha=1}^{q} \iota\left(\frac{\partial \xi_{\kappa}}{\partial u^{\alpha}}\right)\nu^{\kappa} \wedge \vartheta^{\alpha} \tag{2.21}$$

The terms in (2.21) involving wedge products of horizontal and vertical terms are

$$d_{\mathcal{V}}\varpi = \sum_{\kappa=1}^{r}\left[\sum_{\alpha=1}^{q} \iota\left(\frac{\partial \xi_{\kappa}}{\partial u^{\alpha}}\right)\gamma^{\kappa} \wedge \vartheta^{\alpha} + \iota(D\xi_{\kappa})\epsilon^{\kappa} \wedge \varpi\right]. \tag{2.22}$$

Following the same procedure for the invariant contact forms we find

$$d\vartheta^{\alpha}_{J} = d[\iota(\theta^{\alpha}_{J})] = \iota(d\theta^{\alpha}_{J}) + \sum_{\kappa=1}^{r} \nu^{\kappa} \wedge \iota[\mathbf{v}_{\kappa}(\theta^{\alpha}_{J})] = \iota\left(dx \wedge \theta^{\alpha}_{J+1}\right) + \sum_{\kappa=1}^{r} \nu^{\kappa} \wedge \iota\left(\psi^{\alpha}_{J\kappa}\right), \tag{2.23}$$

where

$$\psi^{\alpha}_{J\kappa} = \mathbf{v}_{\kappa}\left(\theta^{\alpha}_{J}\right) = d_{V}\phi^{\alpha}_{Jk} - u^{\alpha}_{J+1}d_{V}\xi_{\kappa}$$

is the vertical prolongation coefficient of the vector field $\mathbf{v}_{\kappa}$. We only need the invariant horizontal component of (2.23) which is

$$d_{\mathcal{H}}\vartheta^{\alpha}_{J} = \varpi \wedge \vartheta^{\alpha}_{J+1} + \sum_{\kappa=1}^{r} \gamma^{\kappa} \wedge \iota(\psi^{\alpha}_{J\kappa}). \tag{2.24}$$

Since

$$d_{\mathcal{H}}\vartheta^{\alpha}_{J} = \varpi \wedge \mathcal{D}\vartheta^{\alpha}_{J}$$

for any contact form ϑ^{α}_{J}, we arrive at the following recurrence relation

$$\mathcal{D}\vartheta^{\alpha}_{J} = \vartheta^{\alpha}_{J+1} + \sum_{\kappa=1}^{r} R^{\kappa}\iota(\psi^{\alpha}_{J\kappa}). \tag{2.25}$$

Using this formula we can write the higher order invariant contact forms as invariant differential operators applied to the order zero invariant contact forms,

$$\vartheta^\alpha_J = \sum_{\beta=1}^{q} \mathcal{E}^\alpha_{J,\beta}(\vartheta^\beta) = \mathcal{E}^\alpha_J(\vartheta). \tag{2.26}$$

Here ϑ is a column vector $(\vartheta^1, ..., \vartheta^q)^T$ made up of the order zero invariant contact forms and $\mathcal{E}^\alpha_J$ is a row vector of order $\#J$ invariant differential operators $(\mathcal{E}^\alpha_{J,1}, ..., \mathcal{E}^\alpha_{J,q})$.

Combining equations (2.20) and (2.26), we can write the invariant vertical derivative of any differential invariant in terms of invariant differential operators applied to the order zero invariant contact forms,

$$d_{\mathcal{V}} K = \mathcal{A}_K(\vartheta) = \sum_{\alpha=1}^{q} \mathcal{A}_{K,\alpha}(\vartheta^\alpha). \tag{2.27}$$

The row vector of q invariant differential operators $\mathcal{A}_K = (\mathcal{A}_{I,1}, ..., \mathcal{A}_{I,q})$ is known as the invariantized Eulerian operator associated with K.

Definition The *Eulerian operator* of a differential invariant K is the invariant differential operator $\mathcal{A}_K$ that satisfies $d_{\mathcal{V}} K = \mathcal{A}_K(\vartheta)$.

Combining (2.17),(2.22), and (2.25), we produce the formula

$$d_{\mathcal{V}} \varpi = \sum_{\alpha=1}^{q} \mathcal{B}_\alpha(\vartheta^\alpha) \wedge \varpi = \mathcal{B}(\vartheta) \wedge \varpi \tag{2.28}$$

for the vertical differentials of the invariant horizontal forms, in which $\mathcal{B}$ is a row vector valued invariant differential operator with q entries known as the invariant Hamiltonian operator complex, again stemming from its role in the invariant calculus of variations.

2.4.3 Recurrence relations for the Euclidean group action

Example Euclidean group acting on curves in $\mathbb{R}^2$

The vector fields

$$\mathbf{v}_1 = \partial_x, \quad \mathbf{v}_2 = \partial_u, \quad \mathbf{v}_3 = -u\partial_x + x\partial_u + (1+u_x^2)\partial_{u_x} + 3u_x u_{xx}\partial_{u_{xx}} + ... \quad (2.29)$$

form a basis for the prolonged infinitesimal generators of the planar Euclidean group action on $\mathbf{R}^2$. To establish the recurrence formulae we need to find the invariantized Maurer-Cartan forms ν^1, ν^2, ν^3 dual to (2.29) by solving the phantom recurrence relations

$$0 = dH = d\iota(x) = \iota(dx) + \sum_{j=1}^{3} \nu^j \iota[\mathbf{v}_j(x)] = \varpi + \nu^1$$

$$0 = dI_0 = d\iota(u) = \iota(u_x dx + \theta) + \sum_{j=1}^{3} \nu^j \iota[\mathbf{v}_j(u)] = \vartheta + \nu^2$$

$$0 = dI_1 = d\iota(u_x) = \iota(u_{xx} dx + \theta_x) + \sum_{j=1}^{3} \nu^j \iota[\mathbf{v}_j(u_x)] = \kappa\varpi + \vartheta^1 + \nu^3.$$

The Maurer-Cartan forms are

$$\nu^1 = -\varpi, \quad \nu^2 = -\vartheta, \quad \nu^3 = -\kappa\varpi - \vartheta^1; \quad (2.30)$$

the Maurer-Cartan invariants are

$$R^1 = -1, \quad R^2 = 0, \quad R^3 = -\kappa = -I_2.$$

Substituting (2.30) into the higher order recurrence relations

$$dI_k = d\iota(u_k) = \iota(u_{k+1} dx + \theta_k) + \sum_{j=1}^{3} \nu^j \iota[\mathbf{v}_j(u_k)] = I_{k+1}\varpi + \vartheta_k - \iota(\varphi_3^k)(\kappa\varpi + \vartheta_1)$$

will prescribe their invariant horizontal differentials

$$d_{\mathcal{H}} I_k = (\mathcal{D} I_k)\varpi = (I_{k+1} - \iota(\varphi_3^k)\kappa)\varpi.$$

The first few invariant derivatives are

$$\mathcal{D} I_2 = I_3, \quad \mathcal{D} I_3 = I_4 - 3I_2^3, \quad \mathcal{D} I_4 = I_5 - 10 I_2^2 I_3.$$

These can be iteratively solved to produce the explicit formulae

$$I_2 = \kappa, \quad I_3 = \kappa_s, \quad I_4 = \kappa_{ss} + 3\kappa^3, \quad I_5 = \kappa_{sss} + 19\kappa^2\kappa_s.$$

The invariant vertical differentials are

$$d_{\mathcal{V}} I_2 = \vartheta_2, \quad d_{\mathcal{V}} I_3 = \vartheta_3 - 3\kappa^2\vartheta_1, \quad d_{\mathcal{V}} I_4 = \vartheta_4 - 10\kappa\kappa_s\vartheta_1. \tag{2.31}$$

Next we compute the invariant derivatives of the invariant contact forms

$$\mathcal{D}\vartheta_k = \vartheta_{k+1} + \sum_{j=1}^{3} R^j \iota(\psi_{k,j}) = \vartheta_{k+1} - \iota(\psi_{k,1}) - \kappa\iota(\psi_{k,3})$$

where the vertical prolongation coefficients $\psi_{k,j} = \mathbf{v}_j(\theta_k)$ are

$$\begin{aligned}
&\psi_{k,1} = \psi_{k,2} = 0\\
&\psi_{0,3} = \mathbf{v}_3(\theta) = u_x\theta,\\
&\psi_{1,3} = \mathbf{v}_3(\theta_x) = 2u_x\theta_x + u_{xx}\theta,\\
&\psi_{2,3} = \mathbf{v}_3(\theta_{xx}) = 3u_x\theta_{xx} + 3u_{xx}\theta_x + u_{xxx}\theta,
\end{aligned}$$

and so on. In particular,

$$\mathcal{D}\vartheta = \vartheta_1, \quad \mathcal{D}\vartheta_1 = \vartheta_2 - \kappa^2\vartheta,$$

$$\mathcal{D}\vartheta_2 = \vartheta_3 - 3\kappa^2\vartheta_1 - \kappa\kappa_s\vartheta, \quad \mathcal{D}\vartheta_3 = \vartheta_4 - 6\kappa^2\vartheta_2 - 4\kappa\kappa_s\vartheta_1 - (\kappa\kappa_{ss} + 3\kappa^4)\vartheta.$$

We recursively solve for ϑ_k

$$\vartheta_1 = \mathcal{D}\vartheta, \quad \vartheta_2 = (\mathcal{D}^2 + \kappa^2)\vartheta, \quad \vartheta_3 = (\mathcal{D}^3 + 4\kappa^2\mathcal{D} + 3\kappa\kappa_s)\vartheta,$$

$$\vartheta_4 = (\mathcal{D}^4 + 10\kappa^2\mathcal{D}^2 + 15\kappa\kappa_s\mathcal{D} + 4\kappa\kappa_{ss} + 3\kappa_s^2 + 9\kappa^4)\vartheta$$

Combining (2.31) and (2.4.3) we find

$$\begin{aligned}
d_{\mathcal{V}}\kappa &= d_{\mathcal{V}} I_2 = (\mathcal{D}^2 + \kappa^2)\vartheta,\\
d_{\mathcal{V}}\kappa_s &= d_{\mathcal{V}} I_3 = (\mathcal{D}^3 + \kappa^2\mathcal{D} + 3\kappa\kappa_s)\vartheta,\\
d_{\mathcal{V}} I_4 &= (\mathcal{D}^4 + 10\kappa^2\mathcal{D}^2 + 5\kappa\kappa_s\mathcal{D} + 4\kappa\kappa_{ss} + 3\kappa_s^2 + 9\kappa^4)\vartheta\\
d_{\mathcal{V}}\kappa_{ss} &= d_{\mathcal{V}} I_4 - 9\kappa^2 d_{\mathcal{V}}\kappa = (\mathcal{D}^4 + \kappa^2\mathcal{D}^2 + 5\kappa\kappa_s\mathcal{D} + 4\kappa\kappa_{ss} + 3\kappa_s^2)\vartheta.
\end{aligned}$$

Thus the Eulerian operators associated to κ,κ_s,κ_{ss} are

$$\mathcal{A}_\kappa = \mathcal{D}^2+\kappa^2, \quad \mathcal{A}_{\kappa_s} = \mathcal{D}^3+\kappa^2\mathcal{D}+3\kappa\kappa_s, \quad \mathcal{A}_{\kappa_{ss}} = \mathcal{D}^4+\kappa^2\mathcal{D}^2+5\kappa\kappa_s\mathcal{D}+4\kappa\kappa_{ss}+3\kappa_s^2. \tag{2.32}$$

Finally we find

$$d\varpi = d[\iota(dx)] = \iota(d^2x)+\sum_{j=1}^{3}\nu^j\wedge\iota[\mathbf{v}_j(dx)] = (-\kappa\varpi-\vartheta_1)\wedge(\vartheta) = -\kappa\vartheta\wedge\varpi+\vartheta_1\wedge\vartheta.$$

This differential breaks up into

$$d_{\mathcal{V}}\varpi = -\kappa\vartheta\wedge\varpi, \quad d_{\mathcal{W}}\varpi = \vartheta_1\wedge\vartheta,$$

and hence the invariant Hamiltonian operator is

$$\mathcal{B} = -\kappa.$$

Higher order linearization operators can be found using the following recurrence.

Lemma 2.14 *For any differential invariant K and any $n \geq 0$,*

$$\mathcal{A}_{\mathcal{D}^nK} = \mathcal{D}^n\circ\mathcal{R}_K + (\mathcal{D}^{n+1}K)\mathcal{D}^{-1}\mathcal{B},$$

where

$$\mathcal{R}_K = \mathcal{A}_K - (\mathcal{D}K)\mathcal{D}^{-1}\mathcal{B}$$

will be called the characteristic operator associated with the differential invariant K.

2.4.4 Recurrence relations for the equi-affine group action

The equi-affine group is defined as the group of area preserving actions on $\mathbb{R}^2$. They can be represented as

$$\begin{pmatrix} y \\ v \end{pmatrix} = A\begin{pmatrix} x \\ u \end{pmatrix} + \begin{pmatrix} a \\ b \end{pmatrix}$$

where $detA = 1$. The infinitesimal generators of the planar equi-affine group are

$$\mathbf{v}_1 = \partial_x, \quad \mathbf{v}_2 = \partial_u, \quad \mathbf{v}_3 = x\partial u, \quad \mathbf{v}_4 = x\partial_x - u\partial_u, \quad \mathbf{v}_5 = u\partial_x.$$

We pick the following cross-section

$$\iota(x) = H = 0,\ \iota(u) = I_0 = 0,\ \iota(u_x) = I_1 = 0,\ \iota(u_{xx}) = I_2 = 1,$$

$$\iota(u_{xxx}) = I_3 = 0,\ \iota(u_{xxxx}) = \kappa = I_4.$$

Picking $u_{xx} = 0$ does not give a cross-section to the group orbits. The first differential invariant $\iota(u_{xxxx})$ is given by

$$\kappa = \frac{3u_{xx}u_{xxxx} - 5u_{xxx}^2}{9u_{xx}^{8/3}} \tag{2.33}$$

and the affine arc length element is given as

$$ds = u_{xx}^{1/3}dx.$$

The corresponding invariant differential operator is

$$D_s = \frac{1}{u_{xx}^{1/3}}D_x.$$

Applying the prolongation of the vector fields in (2.4.4) to $x, u, u_x, u_{xx}, u_{xxx}$ gives

	$\mathbf{v}_1$	$\mathbf{v}_2$	$\mathbf{v}_3$	$\mathbf{v}_4$	$\mathbf{v}_5$
x	1	0	0	0	x
u	0	1	0	0	u
u_x	0	u	1	0	0
u_{xx}	x	$-u$	$-2u_x$	$-3u_{xx}$	$-4u_{xxx}$
u_{xxx}	u	0	$-u_x^2$	$-3u_xu_{xx}$	$-3u_{xx}^2 - 4u_xu_{xxx}$

and we invariantize this table to get

	$\mathbf{v}_1$	$\mathbf{v}_2$	$\mathbf{v}_3$	$\mathbf{v}_4$	$\mathbf{v}_5$
x	1	0	0	0	0
u	0	1	0	0	0
u_x	0	0	1	0	0
u_{xx}	0	0	0	-3	0
u_{xxx}	0	0	0	0	-3.

Applying (2.18) to the phantom invariants we find

$$\begin{aligned}
0 &= d\iota(x) = dy + \nu^1 \\
0 &= d\iota(u) = dv + \nu^2 \\
0 &= d\iota(u_x) = dv_y + \nu^3 \\
0 &= d\iota(u_{xx}) = dv_{yy} - 3\nu^4 \\
0 &= d\iota(u_{xxx}) = dv_{yyy} - 3\nu^5.
\end{aligned}$$

This leads us to the Maurer-Cartan forms

$$\begin{aligned}
\nu^1 &= -dy = -\varpi \\
\nu^2 &= -dv = -v_1\varpi - \vartheta = -\vartheta \\
\nu^3 &= -dv_y = -v_{yy}\varpi - \vartheta = -\varpi - \vartheta_1 \\
\nu^4 &= \frac{1}{3}dv_{yy} = \frac{1}{3}(v_{yyy}\varpi + \vartheta_2) = \frac{1}{3}\vartheta_2 \\
\nu^5 &= \frac{1}{3}dv_{yyy} = \frac{1}{3}(v_{yyyy}\varpi + \vartheta_3) = \frac{1}{3}(I_4\varpi + \vartheta_3).
\end{aligned}$$

From this list we can read off the Maurer-Cartan invariants

$$R^1 = -1, \quad R^2 = 0, \quad R^3 = -1, \quad R^4 = 0, \quad R^5 = \frac{I_4}{3}.$$

The non-zero coefficients related to the vertical forms are

$$S^2_0 = -1, \quad S^3_1 = -1, \quad S^4_2 = \frac{1}{3}, \quad S^5_3 = \frac{1}{3}.$$

We call the first non-constant differential invariant $\kappa = I_4$ and we find the horizontal derivatives

$$\begin{aligned} d_{\mathcal{H}} I_4 &= I_5 \varpi \\ d_{\mathcal{H}} I_5 &= \left(I_6 - 5I_4^2\right) \varpi \\ \mathcal{D} I_4 &= I_5 \\ \mathcal{D} I_5 &= I_6 - 5I_4^2 \\ I_5 &= \mathcal{D} I_4 = \kappa_s \\ I_6 &= \mathcal{D} I_5 + 5I_4^2 = \mathcal{D}^2 I_4 + 5I_4^2 = \kappa_{ss} + 5\kappa^2. \end{aligned}$$

The vertical derivatives of the differential invariants are

$$\begin{aligned} d_{\mathcal{V}} I_4 &= \vartheta_4 + \frac{-5}{3} I_4 \vartheta_2 \\ d_{\mathcal{V}} I_5 &= \vartheta_5 - 2I_5 \vartheta_2 - 5I_4 \vartheta_3. \end{aligned}$$

To find the Eulerian operators associated with I_4, I_5 we must invariantly differentiate the contact forms. The invariant derivative of the invariant contact forms is given by

$$\mathcal{D}\vartheta_k = \vartheta_{k+1} + \sum_{j=1}^{5} R^j \iota(\psi_{k,j}) = \vartheta_{k+1} - \iota(\psi_{k,1}) - \iota(\psi_{k,3}) + \frac{\kappa}{3}\iota(\psi_{k,5})$$

where

$$\begin{aligned} \theta_k &= du_k - u_{k+1} dx \\ \psi_{k,j} &= \mathbf{v}_j(\theta_k) \\ \psi_{k,1} = \psi_{k,2} &= \psi_{k,3} = 0. \end{aligned}$$

Now we must find $\psi_{k,4}, \psi_{k,5}$

	$\mathbf{v}_4$	$\mathbf{v}_5$
θ_0	$-\theta_0$	$-u_x\theta_0$
θ_1	$-2\theta_1$	$-u_{xx}\theta_0 - 2u_x\theta_1$
θ_2	$-3\theta_2$	$-u_{xxx}\theta_0 - 3u_{xx}\theta_1 - 3u_x\theta_2$
θ_3	$-4\theta_3$	$-u_{xxxx}\theta_0 - 4u_{xxx}\theta_1 - 6u_{xx}\theta_2 - 4u_x\theta_3$
θ_4	$-5\theta_4$	$-u_{xxxxx}\theta_0 - 5u_{xxxx}\theta_1 - 10u_{xxx}\theta_2 - 10u_{xx}\theta_3 - 5u_x\theta_4.$

We invariantize this table to find $\iota(\psi_{k,4}), \iota(\psi_{k,5})$

	$\mathbf{v}_4$	$\mathbf{v}_5$
θ_0	$-\vartheta_0$	0
θ_1	$-2\vartheta_1$	$-1\vartheta_0$
θ_2	$-3\vartheta_2$	$-3\vartheta_1$
θ_3	$-4\vartheta_3$	$-I_4\vartheta_0 - 6\vartheta_2$
θ_4	$-5\vartheta_4$	$-I_5\vartheta_0 - 5I_4\vartheta_1 - 10\vartheta_3$.

The recursion formula (2.4.4) further simplifies to $\mathcal{D}\vartheta_k = \vartheta_{k+1} + \frac{\kappa}{3}\iota(\psi_{k,5})$. Now we differentiate the invariant contact forms

$$\begin{aligned}
\mathcal{D}\vartheta_0 &= \vartheta_1 \\
\mathcal{D}\vartheta_1 &= \vartheta_2 - \frac{I_4}{3}\vartheta_0 \\
\mathcal{D}\vartheta_2 &= \vartheta_3 - I_4\vartheta_1 \\
\mathcal{D}\vartheta_3 &= \vartheta_4 - \frac{I_4^2}{3}\vartheta_0 - 2I_4\vartheta_2 \\
\mathcal{D}\vartheta_4 &= \vartheta_5 - \frac{I_5 I_4}{3}\vartheta_0 - \frac{5I_4^2}{3}\vartheta_1 - \frac{10I_4}{3}\vartheta_3.
\end{aligned}$$

The invariant vertical contact forms, ϑ_j, can be recursively solved for

$$\begin{aligned}
\vartheta_1 &= \mathcal{D}\vartheta_0 \\
\vartheta_2 &= \mathcal{D}\vartheta_1 + \frac{\kappa}{3}\vartheta_0 = \left(\mathcal{D}^2 + \frac{\kappa}{3}\right)\vartheta_0 \\
\vartheta_3 &= \left(\mathcal{D}^3 + \frac{4\kappa}{3}\mathcal{D} + \frac{\kappa_s}{3}\right)\vartheta_0 \\
\vartheta_4 &= \left(\mathcal{D}^4 + \frac{10}{3}\kappa\mathcal{D}^2 + \frac{5}{3}\kappa_s\mathcal{D} + \frac{1}{3}\left(\kappa_{ss} + 3\kappa^2\right)\right)\vartheta_0 \\
\vartheta_5 &= \mathcal{D}\vartheta_4 + \frac{\kappa}{3}\left(\kappa_s\vartheta_0 + 5\kappa\vartheta_1 + 10\vartheta_3\right). \\
\vartheta_5 &= \left(\mathcal{D}^5 + \frac{20\kappa}{3}\mathcal{D}^3 + 5\kappa_s\mathcal{D}^2 + \left(2\kappa_{ss} + \frac{64\kappa^2}{9}\right)\mathcal{D} + \frac{\kappa_{sss}}{3} + \frac{31\kappa\kappa_s}{9}\right)\vartheta_0.
\end{aligned}$$

The invariant vertical derivatives of the non-phantom invariants are

$$d_v\kappa = \left(D^4 + \frac{5\kappa}{3}D^2 + \frac{5\kappa_s}{3}D + \frac{1}{3}\kappa_{ss} + \frac{4}{9}\kappa^2\right)\vartheta_0,$$

$$d_v\kappa_s = \left(D^5 + \frac{5\kappa}{3}D^3 + 3\kappa_s D^2 + \left(2\kappa_{ss} + \frac{4}{9}\kappa^2\right)D + \frac{1}{3}\kappa_{sss} + \frac{10}{9}\kappa\kappa_s\right)\vartheta_0,$$

$$\mathcal{A}_\kappa = D^4 + \frac{5\kappa}{3}D^2 + \frac{5\kappa_s}{3}D + \frac{1}{3}\kappa_{ss} + \frac{4}{9}\kappa^2,$$

$$\mathcal{A}_{\kappa_s} = D^5 + \frac{5\kappa}{3}D^3 + 3\kappa_s D^2 + \left(2\kappa_{ss} + \frac{4}{9}\kappa^2\right)D + \frac{1}{3}\kappa_{sss} + \frac{10}{9}\kappa\kappa_s.$$

This gives us the first two Eulerian operators. The differential of the invariant horizontal form is

$$d\varpi = \frac{1}{3}\left(\varpi \wedge (\kappa\vartheta_0 - \vartheta_2) - \vartheta_0 \wedge \vartheta_3\right)$$

which breaks up into the vertical derivative

$$d_{\mathcal{V}}\varpi = \frac{1}{3}\left(\varpi \wedge (\kappa\vartheta_0 - \vartheta_2)\right)$$

and

$$d_{\mathcal{W}}\varpi = \frac{-1}{3}\left(\vartheta_0 \wedge \vartheta_3\right).$$

The invariant Hamiltonian operator is defined by (2.28)

$$\begin{aligned} d_{\mathcal{V}}\varpi &= \frac{1}{3}(\vartheta_2 - \kappa\vartheta_0) \wedge \varpi \\ &= \frac{1}{3}\left(\mathcal{D}^2 + \frac{\kappa}{3} - \kappa\right)\vartheta \wedge \varpi. \end{aligned}$$

The Hamiltonian operator is

$$\mathcal{B} = \frac{1}{3}\left(\mathcal{D}^2 - \frac{2\kappa}{3}\right).$$

The recurrence formula (2.14) can be used to find the the higher order Eulerian operators.

2.4.5 Recurrence relations for the similarity group action

Next we consider invariant flows under the similarity group. This transformation group includes the Euclidean transformations of translation and rotation, and it also includes uniform scaling. The infinitesimal generators of the group action are

$$\mathbf{v}_1 = \partial_x, \quad \mathbf{v}_2 = \partial_u, \quad \mathbf{v}_3 = x\partial_u - u\partial_x, \quad \mathbf{v}_4 = u\partial_u + x\partial x.$$

We pick the cross section

$$0 = H = \iota(x),\ 0 = I_0 = \iota(u),\ 0 = I_1 = \iota(u_1),\ 1 = I_2 = \iota(u_{xx}), \kappa = I_3 = \iota(u_{xxx}).$$

The Lie derivatives of the infinitesimal generators against the coordinates are

	$\mathbf{v}_1$	$\mathbf{v}_2$	$\mathbf{v}_3$	$\mathbf{v}_4$
x	1	0	$-u$	x
u	0	1	x	u
u_x	0	0	$1 + {u_x}^2$	0
u_{xx}	0	0	$3\,u_x u_{xx}$	$-u_{xx}$
u_{xxx}	0	0	$4\,u_x u_{xxx} + 3\,{u_{xx}}^2$	$-2\,u_{xxx}$
u_{xxxx}	0	0	$10\,u_{xx}u_{xxx} + 5\,u_x u_{xxxx}$	$-3\,u_{xxxx}$

and the invariantized version of this table with respect to our cross-section is

	$\mathbf{v}_1$	$\mathbf{v}_2$	$\mathbf{v}_3$	$\mathbf{v}_4$
x	1	0	0	0
u	0	1	0	0
u_x	0	0	1	0
u_{xx}	0	0	0	-1
u_{xxx}	0	0	3	$-2\,I_3$
u_{xxxx}	0	0	$10\,I_3$	$-3\,I_4$.

The differentials of the phantom invariants are

$$\begin{aligned} d\iota(x) &= dy + \nu^1 \\ d\iota(u) &= dv + \nu^2 \\ d\iota(u_x) &= dv_y + \nu^3 \\ d\iota(u_{xx}) &= dv_{yy} - \nu^4. \end{aligned}$$

Solving for the Maurer-Cartan forms we find

$$\begin{aligned}
\nu^1 &= -dy = -\varpi \\
\nu^2 &= -dv = -v_y\varpi - \vartheta_0 = \vartheta_0 \\
\nu^3 &= -dv_y = -v_{yy}\varpi - \vartheta_1 = -\varpi - \vartheta_1 \\
\nu^4 &= dv_{yy} = v_{yyy}\varpi + \vartheta_2 = I_3\varpi + \vartheta_2.
\end{aligned}$$

From here we read off the Maurer-Cartan invariants

$$R^1 = -1, \quad R^2 = 0, \quad R^3 = -1, \quad R^4 = I_3$$

and the other coefficients

$$S_0^2 = 1, \quad S_1^3 = -1, \quad S_2^4 = 1.$$

Now we can find the invariant derivatives of the non-constant invariants

$$\begin{aligned}
\mathcal{D}I_3 &= I_4 - 2I_3^2 - 3I_2 = I_4 - 2I_3^2 - 3 \\
\mathcal{D}I_4 &= I_5 - 3I_4I_3 - 10I_3 \\
I_4 &= \mathcal{D}I_3 + 2I_3^2 + 3 = \kappa_s + 2\kappa^2 + 3 \\
I_5 &= \mathcal{D}I_4 + 3I_4I_3 + 10I_3 = \mathcal{D}^2I_3 + 7I_3\mathcal{D}I_3 + 6I_3^3 + 19I_3 \\
&= \kappa_{ss} + 7\kappa\kappa_s + 6\kappa^3 + 19\kappa.
\end{aligned}$$

To find the derivatives of the vertical invariant forms we must calculate $\psi_{k,j} = \mathbf{v}_j(\theta_k)$

	$\mathbf{v}_1$	$\mathbf{v}_2$	$\mathbf{v}_3$	$\mathbf{v}_4$
θ_0	0	0	$u_1\,\vartheta_0$	ϑ_0
θ_1	0	0	$u_2\,\vartheta_0 + 2\,u_1\,\vartheta_1$	0
θ_2	0	0	$u_3\,\vartheta_0 + 3\,u_2\,\vartheta_1 + 3\,u_1\,\vartheta_2$	$-\,\vartheta_2$
θ_3	0	0	$u_4\,\vartheta_0 + 4\,u_3\,\vartheta_1 + 6\,u_2\,\vartheta_2 + 4\,u_1\,\vartheta_3$	$-2\,\vartheta_3$
θ_4	0	0	$u_5\,\vartheta_0 + 5\,u_4\,\vartheta_1 + 10\,u_3\,\vartheta_2 + 10\,u_2\,\vartheta_3 + 5\,u_1\,\vartheta_4$	$-3\,\vartheta_4$
θ_5	0	0	$u_6\,\vartheta_0 + 6\,u_5\,\vartheta_1 + 15\,u_4\,\vartheta_2 + 20\,u_3\,\vartheta_3 + 15\,u_2\,\vartheta_4 + 6\,u_1\,\vartheta_5$	$-4\,\vartheta_5$.

The invariantized version of this table is

	$\mathbf{v}_1$	$\mathbf{v}_2$	$\mathbf{v}_3$	$\mathbf{v}_4$
θ_0	0	0	0	ϑ_0
θ_1	0	0	ϑ_0	0
θ_2	0	0	$I_3\,\vartheta_0 + 3\,\vartheta_1$	$-\vartheta_2$
θ_3	0	0	$I_4\,\vartheta_0 + 4\,I_3\,\vartheta_1 + 6\,\vartheta_2$	$-2\,\vartheta_3$
θ_4	0	0	$I_5\,\vartheta_0 + 5\,I_4\,\vartheta_1 + 10\,I_3\,\vartheta_2 + 10\,\vartheta_3$	$-3\,\vartheta_4$
θ_5	0	0	$I_6\,\vartheta_0 + 6\,I_5\,\vartheta_1 + 15\,I_4\,\vartheta_2 + 20\,I_3\,\vartheta_3 + 15\,\vartheta_4$	$-4\,\vartheta_5$.

Next we invariantly differentiate the invariant vertical forms

$$\begin{aligned}
\mathcal{D}\vartheta_0 &= \vartheta_1 + \kappa\vartheta_0\\
\mathcal{D}\vartheta_1 &= \vartheta_2 - \vartheta_0\\
\mathcal{D}\vartheta_2 &= \vartheta_3 - \kappa\vartheta_0 - 3\vartheta_1 - \kappa\vartheta_2\\
\mathcal{D}\vartheta_3 &= \vartheta_4 - I_4\vartheta_0 - 4\kappa\vartheta_1 - 6\vartheta_2 - 2\kappa\vartheta_3
\end{aligned}$$

and solve for ϑ_1,ϑ_2,ϑ_3 in terms of derivatives of ϑ_0

$$\begin{aligned}
\vartheta_1 &= \mathcal{D}\vartheta_0 - \kappa\vartheta_0\\
\vartheta_2 &= \mathcal{D}\vartheta_1 + \vartheta_0 = \left(\mathcal{D}^2 - \kappa_s - \kappa\mathcal{D} + 1\right)\vartheta_0\\
\vartheta_3 &= \mathcal{D}\vartheta_2 + \kappa\vartheta_0 + 3\vartheta_1 + \kappa\vartheta_2 = \left(\mathcal{D}^3 + (-\kappa^2 - 2\kappa_s + 4)\mathcal{D} - \kappa_{ss} - \kappa\kappa_s - 2\kappa\right)\vartheta_0.
\end{aligned}$$

Using these we find the vertical derivative of κ and the Eulerian operator associated to κ

$$\begin{aligned}
d_{\mathcal{V}} I_3 &= -3\vartheta_1 - 2\kappa\vartheta_2 + \vartheta_3\\
&= \left(\mathcal{D}^3 - 2\kappa\mathcal{D}^2 + (\kappa^2 - 2\kappa_s + 1)\mathcal{D} - \kappa_{ss} + \kappa\kappa_s - \kappa\right)\vartheta_0\\
\mathcal{A}_\kappa &= \mathcal{D}^3 - 2\kappa\mathcal{D}^2 + (\kappa^2 - 2\kappa_s + 1)\mathcal{D} - \kappa_{ss} + \kappa\kappa_s - \kappa.
\end{aligned}$$

To find the Hamiltonian operator we take the vertical derivative of ϖ

$$d_{\mathcal{V}}\varpi = (\vartheta_2 - \vartheta_0) \wedge \varpi = (\mathcal{D}^2 - \kappa\mathcal{D} - \kappa_s)\vartheta_0 \wedge \varpi = \mathcal{B}\,(\vartheta_0) \wedge \varpi$$

$$\mathcal{B} = (\mathcal{D}^2 - \kappa\mathcal{D} - \kappa_s).$$

2.4.6 Recurrence relations for the centro-affine group acting on space curves

To go along with the various planar group actions we include one action on space curves, the centro-affine action. The transformation is given by

$$\begin{bmatrix} y \\ v^1 \\ v^2 \end{bmatrix} = A \begin{bmatrix} x \\ u^1 \\ u^2 \end{bmatrix}, \qquad det(A) = 1.$$

The matrix A has nine entries and with the restriction on the determinant the matrices form an 8-parameter group. We parameterize this group using the variables $(a_1, a_2, a_3, a_4, a_5, a_6, a_7, a_8)$ where the matrix A is given as

$$A = \begin{bmatrix} a_0 & a_1 & a_2 \\ a_3 & 1+a_4 & a_5 \\ a_6 & a_7 & 1+a_8 \end{bmatrix},$$

where a_0 is determined by $det(A) = 1$. This particular parameterization was chosen so that the transformation related to $(a_1, a_2, ..., a_8) = (0, 0, ..., 0)$ is the identity. The vector fields that generate this group action are

$$\begin{aligned} \mathbf{v}_1 &= u^1 \partial x & \mathbf{v}_2 &= u^2 \partial x \\ \mathbf{v}_3 &= x \partial u^1 & \mathbf{v}_4 &= u^1 \partial u^1 - x \partial x \\ \mathbf{v}_5 &= u^2 \partial u^1 & \mathbf{v}_6 &= x \partial u^2 \\ \mathbf{v}_7 &= u^1 \partial u^2 & \mathbf{v}_8 &= u^2 \partial u^2 - x \partial x. \end{aligned}$$

We have picked the following cross-section coordinates for our normalization

$$H = 0 \qquad I^1 = 0 \qquad I^2 = 1$$

$$I^1_1 = 0 \qquad I^2_1 = 0$$

$$I^1_2 = 1 \qquad I^2_2 = 0$$

$$I_3^1 = 0 \qquad I_3^2 = \kappa.$$

Our first differential invariant appears at order 3. Generically the rank of this invariant will be 1, so the differential invariant signature is the functional relationship between the invariants $I_3^2 = \kappa, I_4^1 = \tau, \mathcal{D}I_3^2 = \kappa_s$.

We find the Maurer-Cartan forms by differentiating the coordinates of our moving frame

$$\begin{aligned}
0 = dH &= dy + \nu^2 \\
0 = dI^1 &= dv^1 + \nu^5 \\
0 = dI^2 &= dv^2 + \nu^8 \\
0 = dI_1^1 &= dv_1^1 + \nu^3 \\
0 = dI_1^2 &= dv_1^2 + \nu^6 \\
0 = dI_2^1 &= dv_2^1 + 3\nu^4 + 2\nu^8 \\
0 = dI_2^2 &= dv_2^2 + \nu^7 \\
0 = dI_3^1 &= dv_3^1 - 3\nu^1 + v_3^2\nu^5.
\end{aligned}$$

The Maurer-Cartan forms are

$$\begin{aligned}
\nu^2 &= -dy = -\varpi \\
\nu^5 &= -dv^1 = -\vartheta^1 + v_1^1\varpi = -\vartheta^1 \\
\nu^8 &= -dv^2 = -\vartheta^2 - v_1^2\varpi = -\vartheta^2 \\
\nu^3 &= -dv_1^1 = -\vartheta_1^1 - v_2^1\varpi = -\vartheta_1^1 - \varpi \\
\nu^6 &= -dv_1^2 = -\vartheta_1^2 - v_2^2\varpi = -\vartheta_1^2 \\
\nu^4 &= -\frac{dv_2^1 + 2\nu^8}{3} = -\frac{dv_2^1 - 2dv^2}{3} = -\frac{\vartheta_2^1 + v_3^1\varpi - 2\vartheta^2 - 2v_1^2\varpi}{3} \\
&= -\frac{\vartheta_2^1 + (v_3^1 - 2v_1^2)\varpi - 2\vartheta^2}{3} = -\frac{\vartheta_2^1 - 2\vartheta^2}{3} \\
\nu^7 &= -dv_2^2 = -\vartheta_2^2 - v_3^2\varpi = -\vartheta_2^2 - v_3^2\varpi \\
\nu^1 &= \frac{dv_3^1 + v_3^2\nu^5}{3} = \frac{dv_3^1 - v_3^2 dv^1}{3} = \frac{\vartheta_3^1 + v_4^1\varpi - v_3^2(\vartheta^1 + v_1^1\varpi)}{3} \\
&= \frac{\vartheta_3^1 - v_3^2\vartheta^1}{3} + \frac{v_4^1\varpi}{3}.
\end{aligned}$$

From here we can read off the nonzero Maurer-Cartan invariants

$$R^2 = -1, \quad R^3 = -1, \quad R^7 = -v_3^2, \quad R^1 = \frac{v_4^1}{3}$$

and the other vertical invariants

$$S_1^{5,0} = -1, \quad S_2^{8,0} = -1, \quad S_1^{3,1} = -1, \quad S_2^{6,1} = -1,$$

$$S_1^{4,2} = -\frac{1}{3}, \quad S_2^{4,0} = \frac{1}{3}, \quad S_2^{7,2} = -1, \quad S_1^{1,3} = \frac{1}{3}, \quad S_1^{1,0} = -\frac{v_3^2}{3}.$$

The differentials of the differential invariants are

$$\begin{aligned}
dI_3^2 &= -2v_3^2\vartheta^2 - v_3^2\vartheta_2^1 + \vartheta_3^2 + v_4^2\varpi \\
dI_4^1 &= -v_4^2\,\vartheta^1 - \frac{2}{3}\,v_4^1\,\vartheta^2 - \frac{5}{3}\,v_4^1\,\vartheta_2^1 + \,\vartheta_4^1 + (v_5^1 + 4\,v_3^2)\,\varpi \\
dI_4^2 &= 2\,(v_3^2)^2\,\vartheta^1 - \frac{7}{3}\,v_4^2\,\vartheta^2 - \frac{4}{3}\,v_4^2\,\vartheta_2^1 - v_4^1\,\vartheta_2^2 - 2\,v_3^2\,\vartheta_3^1 + \,\vartheta_4^2 + (v_5^2 - 3\,v_4^1 v_3^2)\,\varpi.
\end{aligned}$$

These differentials split into vertical and horizontal components

$$
\begin{aligned}
d_{\mathcal{V}} I_3^2 &= -2v_3^2\vartheta^2 - v_3^2\vartheta_2^1 + \vartheta_3^2 \\
d_{\mathcal{H}} I_3^2 &= v_4^2\varpi \\
d_{\mathcal{V}} I_4^1 &= -v_4^2\,\vartheta^1 - \frac{2}{3}\,v_4^1\,\vartheta^2 - \frac{5}{3}\,v_4^1\,\vartheta_2^1 + \,\vartheta_4^1 \\
d_{\mathcal{H}} I_4^1 &= (v_5^1 + 4\,v_3^2)\,\varpi \\
d_{\mathcal{V}} I_4^2 &= 2\,(v_3^2)^2\,\vartheta^1 - \frac{7}{3}\,v_4^2\,\vartheta^2 - \frac{4}{3}\,v_4^2\,\vartheta_2^1 - v_4^1\,\vartheta_2^2 - 2\,v_3^2\,\vartheta_3^1 + \,\vartheta_4^2 \\
d_{\mathcal{H}} I_4^2 &= (v_5^2 - 3\,v_4^1 v_3^2)\,\varpi.
\end{aligned}
$$

The invariant derivatives are defined via Equation (2.10)

$$
\begin{aligned}
\mathcal{D} I_3^2 &= v_4^2 = \kappa_s \\
\mathcal{D} I_4^1 &= v_5^1 + 4v_3^2 = \tau_s \\
\mathcal{D} I_4^2 &= v_5^2 - 3v_4^1 v_3^2 = \kappa_{ss}.
\end{aligned}
$$

The invariant derivatives of the contact forms are

$$
\begin{aligned}
\mathcal{D}\vartheta^1 &= \vartheta_1^1 \\
\mathcal{D}\vartheta^2 &= -v_3^2\vartheta^1 + \vartheta_1^2 \\
\mathcal{D}\vartheta_1^1 &= -\frac{1}{3}v_4^1\vartheta^1 + \vartheta^2 + \vartheta_2^1 \\
\mathcal{D}\vartheta_1^2 &= -v_3^2\vartheta_1^1 + \vartheta_2^2 \\
\mathcal{D}\vartheta_2^1 &= -v_4^1\vartheta_1^1 + 2\vartheta_1^2 + \vartheta_3^1 \\
\mathcal{D}\vartheta_2^2 &= -\frac{1}{3}v_3^2 v_4^1\vartheta^1 + v_3^2\vartheta^2 - \frac{1}{3}v_4^1\vartheta_1^2 - v_3^2\vartheta_2^1 + \vartheta_3^2 \\
\mathcal{D}\vartheta_3^1 &= -\frac{1}{3}(v_4^1)^2\vartheta^1 + v_4^1\vartheta_0^2 + v_3^2\vartheta_1^1 - 2v_4^1\vartheta_2^1 + 3\vartheta_2^2 + \vartheta_4^1.
\end{aligned}
$$

We now solve for the higher order contact forms

$$
\begin{aligned}
\vartheta_1^1 =& \mathcal{D}\vartheta^1 \\
\vartheta_1^2 =& \mathcal{D}\vartheta^2 + v_3^2\vartheta^1 \\
\vartheta_2^1 =& \mathcal{D}\vartheta_1^1 + \frac{1}{3}v_4^1\vartheta^1 - \vartheta^2 \\
=& \mathcal{D}^2\vartheta^1 + \frac{1}{3}v_4^1\vartheta^1 - \vartheta^2 \\
\vartheta_2^2 =& \mathcal{D}\vartheta_1^2 + v_3^2\vartheta_1^1 = \mathcal{D}^2\vartheta^2 + \mathcal{D}v_3^2\vartheta^1 + 2v_3^2\mathcal{D}\vartheta^1 \\
\vartheta_3^1 =& \mathcal{D}\vartheta_2^1 + v_4^1\vartheta_1^1 - 2\vartheta_1^2 \\
=& \left(\mathcal{D}^3 + \frac{4}{3}v_4^1\mathcal{D} + \frac{1}{3}\mathcal{D}v_4^1 - 2v_3^2\right)\vartheta^1 - 3\mathcal{D}\vartheta^2 \\
\vartheta_3^2 =& \mathcal{D}\vartheta_2^2 + \frac{1}{3}v_3^2v_4^1\vartheta^1 - v_3^2\vartheta^2 + \frac{1}{3}v_4^1\vartheta_1^2 + v_3^2\vartheta_2^1 \\
=& \left(3v_3^2\mathcal{D}^2 + 3\mathcal{D}v_3^2\mathcal{D} + v_3^2v_4^1 + \mathcal{D}^2v_3^2\right)\vartheta^1 \\
&+ \left(\mathcal{D}^3 + \frac{1}{3}v_4^1\mathcal{D} - 2v_3^2\right)\vartheta^2 \\
\vartheta_4^1 =& \mathcal{D}\vartheta_3^1 + \frac{1}{3}(v_4^1)^2\vartheta^1 - v_4^1\vartheta^2 - v_3^2\vartheta_1^1 + 2v_4^1\vartheta_2^1 - 3\vartheta_2^2 \\
=& \left(\mathcal{D}^4 + \frac{10}{3}v_4^1\mathcal{D}^2 + \frac{5}{3}\mathcal{D}v_4^1\mathcal{D} - 9v_3^2\mathcal{D} + \frac{1}{3}\mathcal{D}^2v_4^1 - 5\mathcal{D}v_3^2 + (v_4^1)^2\right)\vartheta^1 \\
&- \left(6\mathcal{D}^2 + 3v_4^1\right)\vartheta^2.
\end{aligned}
$$

We find the Hamiltonian operator using the vertical derivative of ϖ

$$
\begin{aligned}
d_v\varpi &= \frac{1}{3}\,v_4^1\,\varpi\wedge\vartheta^1 - \frac{4}{3}\,\varpi\wedge\vartheta^2 - \frac{1}{3}\,\varpi\wedge\vartheta_2^1 \\
\mathcal{B} &= -\frac{1}{3}v_4^1\vartheta^1 + \frac{4}{3}\vartheta_0^2 + \frac{1}{3}\vartheta_2^1 \\
&= \left(\frac{1}{3}\mathcal{D}^2 - \frac{2}{9}v_4^1\right)\vartheta^1 + \vartheta^2 \\
\mathcal{B}_1 &= \frac{1}{3}\mathcal{D}^2 - \frac{2}{9}v_4^1 \\
\mathcal{B}_2 &= 1.
\end{aligned}
$$

The vertical derivatives of the differential invariants κ, τ are

$$\begin{aligned}
d_{\mathcal{V}} I_3^2 =& \left(2v_3^2\mathcal{D}^2 + 3\mathcal{D}v_3^2\mathcal{D} + \mathcal{D}^2 v_3^2 + \frac{2}{3}v_3^2 v_4^1\right)\vartheta^1 \\
&+ \left(\mathcal{D}^3 + \frac{1}{3}v_4^1\mathcal{D} - 3v_3^2\right)\vartheta^2 \\
d_{\mathcal{V}} I_4^1 =& \left(\mathcal{D}^4 + \frac{5}{3}v_4^1\mathcal{D}^2 + \left(\frac{5}{3}\mathcal{D}(v_4^1) - 9v_3^2\right)\mathcal{D} + \frac{1}{3}\mathcal{D}^2(v_4^1) + \frac{4}{9}(v_4^1)^2 - 6\mathcal{D}(v_3^2)\right)\vartheta^1 \\
&- \left(6\mathcal{D}^2 + 2v_4^1\right)\vartheta^2 \\
\mathcal{A}_{I_3^2,1} =& 2v_3^2\mathcal{D}^2 + 3\mathcal{D}v_3^2\mathcal{D} + \mathcal{D}^2 v_3^2 + \frac{2}{3}v_3^2 v_4^1 \\
=& 2\kappa\mathcal{D}^2 + 3\kappa_s\mathcal{D} + \kappa_{ss} + \frac{2}{3}\kappa\tau \\
\mathcal{A}_{I_3^2,2} =& \mathcal{D}^3 + \frac{1}{3}v_4^1\mathcal{D} - 3v_3^2 \\
=& \mathcal{D}^3 + \frac{1}{3}\tau\mathcal{D} - 3\kappa \\
\mathcal{A}_{I_4^1,1} =& \mathcal{D}^4 + \frac{5}{3}v_4^1\mathcal{D}^2 + \left(\frac{5}{3}\mathcal{D}(v_4^1) - 9v_3^2\right)\mathcal{D} + \frac{1}{3}\mathcal{D}^2(v_4^1) + \frac{4}{9}(v_4^1)^2 - 6\mathcal{D}(v_3^2) \\
=& \mathcal{D}^4 + \frac{5}{3}\tau\mathcal{D}^2 + \left(\frac{5}{3}\tau_s - 9\kappa\right)\mathcal{D} + \frac{1}{3}\tau_{ss} + \frac{4}{9}\tau^2 - 6\kappa_s \\
\mathcal{A}_{I_4^1,2} =& -6\mathcal{D}^2 - 2v_4^1 \\
=& -6\mathcal{D}^2 - 2\tau.
\end{aligned}$$

Using the recursion formula (2.14) we find $\mathcal{A}_{I_4^2}$

$$\begin{aligned}
\mathcal{A}_{I_4^2,1} =& \mathcal{D}\mathcal{A}_{I_3^2,1} - D\, I_3^2\, \mathcal{B}_1 \\
=& \kappa_s\mathcal{D}^2 + \kappa\mathcal{D}^3 + \kappa_{ss} + \kappa_s\mathcal{D} + \frac{1}{3}(\kappa_s\tau + \kappa\tau_s) \\
&- \kappa_s\left(\frac{1}{3}\mathcal{D}^2 - \frac{2}{9}\tau\right) \\
\mathcal{A}_{I_4^2,2} =& \mathcal{D}^4 - 3\mathcal{D}v_3^2 - 3v_3^2\mathcal{D} + \frac{1}{3}\left(\mathcal{D}v_4^1\mathcal{D} + v_4^1\mathcal{D}^2\right) - \mathcal{D}v_3^2 \\
=& \mathcal{D}^4 - 3\kappa_s - 3\kappa\mathcal{D} + \frac{1}{3}\left(\tau_s\mathcal{D} + \tau\mathcal{D}^2\right) - \kappa_s \\
=& \mathcal{D}^4 + \frac{\tau}{3}\mathcal{D}^2 + \left(\frac{\tau_s}{3} - 3\kappa\right)\mathcal{D} - 4\kappa_s.
\end{aligned}$$

2.5 Invariant curve flows

To consider how group actions interact with curve flows, we extend the group action on a manifold to also act on a time variable. The extended group action acts trivially on the time variable. A curve flow is given by the evolutionary partial differential equation

$$\frac{\partial C}{\partial t} = \Phi(C), \tag{2.34}$$

which determines the motion of a one-dimensional submanifold $C \subset M$. Since the extended group action acts trivially on t, equation (2.34) is G-invariant if and only if $\Phi(C)$ is G-invariant. If (2.34) is G-invariant, then its solutions are *invariant curve flows*.

We work with the invariant variational complex to categorize such flows, and to find the evolution of the differential invariants.

First we examine the $m = 1 + q$ invariant one-forms

$$\varpi, \vartheta^1, ..., \vartheta^q, \tag{2.35}$$

each of which is a linear combination of the coordinate one-forms $dx, du_1, ...du_q$ on M. The coefficients are n^{th} order differential invariant functions where n is the order of the underlying moving frame.

Let $C \subset M$ be a smooth 1-dimensional submanifold. Evaluating the coefficients of (2.35) on the submanifold jet $(x, u^{(n)}) = j^n S|_z$ produces a basis for the cotangent space $T^*M|_z$ of the ambient manifold, which we continue to denote by (2.35). By construction, the resulting cotangent space basis is equivariant under the action of G on $C \subset M$.

Let $\mathbf{t}, \mathbf{n}_1, ..., \mathbf{n}_q$ denote the corresponding dual tangent vectors, which form a G-equivariant basis of the bundle $TM \to C$, or frame on C. Since the contact forms annihilate the tangent bundle TC, the vector $\mathbf{t}$ generates the tangent bundle TC while $\mathbf{n}_1, .., \mathbf{n}_q$ form a basis for the complementary G-equivariant normal bundle $NC \to C$ induced by the moving frame.

Example In the case of planar curves we have $p = q = 1$. If we take our transformation group to be the Euclidean group, we have the invariant differential forms:

$$\varpi = \frac{dx + u_x\, du}{\sqrt{1+u_x^2}} = \sqrt{1+u_x^2}\, dx + \frac{u_x}{\sqrt{1+u_x^2}}\, \theta$$
$$\vartheta = \frac{\theta}{\sqrt{1+u_x^2}}.$$

The usual Euclidean frame is given by the unit tangent and normal vectors as calculated in example 2.4.1

$$\mathbf{t} = \frac{1}{\sqrt{1+u_x^2}} \left(\frac{\partial}{\partial x} + u_x \frac{\partial}{\partial u} \right)$$
$$\mathbf{n} = \frac{1}{\sqrt{1+u_x^2}} \left(-u_x \frac{\partial}{\partial x} + \frac{\partial}{\partial u} \right).$$

These vector fields are dual to the invariant differential forms

$$\langle \mathbf{t}, \varpi \rangle = \langle \mathbf{n}, \vartheta \rangle = 1, \quad \langle \mathbf{t}, \vartheta \rangle = \langle \mathbf{n}, \varpi \rangle = 0.$$

In general, let

$$\mathbf{V} = \mathbf{V}|_S = \mathbf{V}_T + \mathbf{V}_N = I\mathbf{t} + \sum_{\alpha=1}^{q} J^\alpha \mathbf{n}_\alpha$$

be a section of the bundle $TM \to C$, where $\mathbf{V}_T, \mathbf{V}_N$ denote its tangential and normal components and I, J^α are differential functions, depending on the submanifold jets. We refer to $\mathbf{V}$ as a vector field despite the fact that it is only defined on C. Any such vector field generates a submanifold flow

$$\frac{\partial C}{\partial t} = \mathbf{V}|_{C(t)}. \tag{2.36}$$

The flow (2.36) defines an n^{th} order system of partial differential equations, where n is the larger of the order of our moving frame and the order of the coefficients I, J^α. Assuming local existence and uniqueness, a solution $C(t)$ to (2.36) defines a smoothly varying family of curves in M. Typically singularities arise if the flow is continued for a sufficiently long time.

Lemma 2.15 *The vector field* $\mathbf{V}$ *generates an invariant submanifold flow if and only if its coefficients* $I = \langle \mathbf{V}; \varpi \rangle$, $J^\alpha = \langle \mathbf{V}; \vartheta^\alpha \rangle$, *are differential invariants.*

The following are a number of examples of Euclidean invariant curve flows.

Example

The flow given by $J = 1$ is called the grassfire or optical flow. It is also closely related to the distance transform.

The flow given by $J = \kappa^{1/3}$ is ,up to a reparameterization of the curve, equivalent to the equi-affine curve flow [47].

The flow given by $J = \kappa$ is the curve shortening flow [24] which is widely used in image processing.

The flow given by $J = \kappa_s$ leads to a modified Korteweg-de Vries equation.

The flow given by $J = -\kappa_{ss}$ also shortens the curve, but it also preserves the area inside the curve. This curve flow has been studied by Cahn and Taylor [11], Cahn, Elliot and Novick-Cohen [10] and Giga and Ito [25]. This flow also models the thermal grooving of metals [8].

Evolution of invariants

Given an invariant submanifold flow we would also like to calculate the evolution of the differential invariants. Let K be any differential invariant and $\mathbf{V}$ be the vector field which generates an intrinsic flow. The time variation of K is found by computing the Lie derivative

$$\mathbf{V}(K) = \mathbf{V} \lrcorner\, dK = \mathbf{V} \lrcorner\, (\mathcal{A}_K(\vartheta) + \mathcal{D}K\varpi) = \mathcal{A}_K(J) + I\,\mathcal{D}K.$$

Theorem 2.16 *If the submanifold flow is intrinsic and* K *is any differential invariant, then*

$$\frac{\partial K}{\partial t} = \mathbf{V}(K) = \mathcal{A}_K(J) + I\mathcal{D}K.$$

The quantity $I\mathcal{D}K$ is exactly the tangential evolution of K due to reparametrization

$$I\mathcal{D}K = (\mathcal{D}K)\mathbf{V} \lrcorner \varpi = \mathbf{V} \lrcorner d_{\mathcal{H}}K.$$

Since the tangential component only reparameterizes the curve, the normal component is the only portion of the flow that effects the geometry of the curve. In fact, we show in section 3.1 that the tangential velocity does not change the differential invariant signature.

Definition Any submanifold flow that can be represented as

$$\frac{\partial C}{\partial t} = \sum_{\alpha=1}^{q} J^{\alpha}\mathbf{n}_{\alpha}$$

is called *normal*.

Theorem 2.17 *If a submanifold flow is normal, and K is any differential invariant, then*

$$\frac{\partial K}{\partial t} = \mathbf{V}(K) = \mathcal{A}_K(J).$$

Example The curve shortening flow is the normal flow given by $J = \kappa$. Using the Eulerian operators (2.32) we can find the evolution of the differential invariants,

$$\frac{\partial \kappa}{\partial t} = \kappa_{ss} + \kappa^3$$

$$\frac{\partial \kappa_s}{\partial t} = \kappa_{sss} + \kappa^2\kappa_s + 3\kappa^2\kappa_s,$$

and so on.

Chapter 3

Evolution of differential invariant signatures

3.1 General framework

In section 2.5 we have laid out all the machinery we need to find the evolution of differential invariants. This leads to an evolutionary equation for each invariant. Since the invariant differential operators generally do not commute with the time derivative we cannot treat these evolutionary equations as traditional partial differential equations (PDE's). Instead of working directly with the invariants we investigate how the signature evolves.

For example, consider the Euclidean action on planar curves. The signature of a plane curve $C \subset \mathbb{R}^2$ is a curve $\Sigma \subset \mathbb{R}^2$ parameterized by (κ, κ_s). A *vertex* is a local extrema of curvature. Any simple closed curve has at least four vertices [42]. The signature will wind around in the (κ, κ_s) plane passing through the κ-axis at least four times. We break up the signature at each vertex and call each portion a *signature segment*. On each segment we can write κ_s as a function of κ:

$$\kappa_s = H(\kappa).$$

By differentiating with respect to the arc length we find

$$\kappa_{ss} = H_\kappa(\kappa)\kappa_s = H_\kappa H, \quad \kappa_{sss} = H_{\kappa\kappa}H^2 + H_\kappa^2 H. \tag{3.1}$$

Higher order invariants can be found by differentiating the right hand side.

Suppose we have a family of planar curves $C(t)$ evolving with a normal velocity given by J and a tangential velocity given by I. This family of curves has a corresponding family of signatures locally given by $\kappa_s = H(\kappa, t)$ where H is a function from $\Gamma = \{(\kappa, t) | a(t) < \kappa < b(t), 0 \leq t \leq T\}$ to $\mathbb{R}$. The functions $a(t), b(t)$ are the values of κ at the two vertices that bound this signature segment. From (2.16) the evolution of κ, κ_s are given by

$$\begin{aligned} \frac{\partial \kappa}{\partial t} &= \mathcal{A}_\kappa(J) + I\kappa_s, \\ \frac{\partial \kappa_s}{\partial t} &= \mathcal{A}_{\kappa_s}(J) + I\kappa_{ss}. \end{aligned}$$

We now differentiate the signature with respect to t to find

$$\begin{aligned} \frac{\partial \kappa_s}{\partial t} &= \frac{\partial H}{\partial t} + \frac{\partial H}{\partial \kappa}\frac{\partial \kappa}{\partial t} \\ \mathcal{A}_{\kappa_s}(J) + I\kappa_{ss} &= \frac{\partial H}{\partial t} + \frac{\partial H}{\partial \kappa}\left(\mathcal{A}_\kappa(J) + I\kappa_s\right) \\ \mathcal{A}_{\kappa_s}(J) + IHH_\kappa &= H_t + H_\kappa \mathcal{A}_\kappa(J) + IHH_\kappa \\ H_t &= \mathcal{A}_{\kappa_s}(J) - H_\kappa \mathcal{A}_\kappa(J). \end{aligned} \tag{3.2}$$

As expected, the evolution of the signature does not depend on the tangential velocity I. Since the signature determines the geometry of the curve, and the tangential velocity does not change the signature, we see that the tangential velocity has no effect on the geometry of the curve. We will ignore any tangential velocities for the remainder of this thesis.

The evolution of the signature is found by combining (3.2) and (3.1). In the case of the curve shortening flow the evolution of the signature is given by

$$H_t = \kappa_{sss} + \kappa^2\kappa_s + 3\kappa^2\kappa_s - H_\kappa(\kappa_{ss} + \kappa^3)$$

$$\frac{\partial H}{\partial t} = H^2 H_{\kappa\kappa} - \kappa^3 H_\kappa + 4\kappa^2 H. \tag{3.3}$$

For the grassfire flow $J = 1$ we have

$$\mathcal{A}_\kappa(1) = \kappa^2 \qquad \mathcal{A}_{\kappa_s}(1) = 3\kappa\kappa_s \qquad H_t = 3\kappa H - H_\kappa \kappa^2.$$

3.1.1 Endpoints of segments

Away from a vertex the evolution of the signature function is given by (3.2), but we are also interested in how the endpoints of the segments evolve. To find the evolution of the endpoints we need to know about the shape of the signature near the endpoints.

Theorem 3.1 *Suppose we have a regular curve. The corresponding signature either consists of a single point, or H_κ is unbounded as we approach a vertex.*

This tells us that the tangent to the signature is vertical at any point where $\kappa_s = 0$.

Proof The signature is the map $\phi : C \to (\kappa, \kappa_s)$. If the rank of the signature is 0 then the signature is a single point. Otherwise the rank of the signature is 1 on the entire curve. At a vertex we have $\kappa_s = 0$ so $\kappa_{ss} \neq 0$, otherwise the rank will be 0, contradicting our assumption that the curve is regular. From (3.1) we have $\kappa_{ss} = H H_\kappa$. Since $H = 0$ and $\kappa_{ss} \neq 0$ at a vertex then H_κ must be unbounded as we approach a vertex.

Motion of endpoints

To study the evolution of the endpoints of a signature segment we set up two functions $a^\delta(t), b^\delta(t)$ which are defined so that $H(a^\delta(t), t) = H(b^\delta(t), t) = \delta$. We pick $a^\delta(0)$ to be the smallest value of κ for which $H(\kappa, 0) = \delta$, and $b^\delta(0)$ to be the largest value of κ for which $H(\kappa, 0) = \delta$. We obtain the evolution of the left and right endpoints by examining the evolution of $a^\delta(t), b^\delta(t)$ as δ to goes to 0. Since

$H(a^\delta(t),t)$ remains constant with respect to t we have

$$\frac{dH(a^\delta(t),t)}{dt} = \left.\frac{\partial H(\kappa,t)}{\partial \kappa}\right|_{(\kappa=a^\delta(t),t=t)} \frac{da^\delta(t)}{dt} + \left.\frac{\partial H(\kappa,t)}{\partial t}\right|_{(\kappa=a^\delta(t),t=t)} = 0.$$

Using this information we find

$$\frac{da^\delta(t)}{dt} = -\frac{\left.\frac{\partial H(\kappa,t)}{\partial t}\right|_{(\kappa=a^\delta(t),t=t)}}{\left.\frac{\partial H(\kappa,t)}{\partial \kappa}\right|_{(\kappa=a^\delta(t),t=t)}} = -\frac{\mathcal{A}_{\kappa_s}(J)}{H_\kappa} + \mathcal{A}_\kappa(J). \tag{3.4}$$

As long as the curve remains regular Theorem 3.1 applies and the quantity H_κ grows unbounded as δ goes to 0. This gives the evolution of the endpoints

$$\lim_{\delta\to 0} \frac{da^\delta(t)}{dt} = \frac{da(t)}{dt} = \mathcal{A}_\kappa(J).$$

The evolution of the endpoints of a signature segment is given just by the evolution of κ, evaluated at that endpoint.

3.2 Evolution of signatures

As shown in section 3.1 the invariant flow of a curve leads to evolutionary equations for the differential invariants and for the differential invariant signature. In this section we explore the evolutionary partial differential equations that arise for the signature. A result from Angenent [4] proves that the number of vertices is non-increasing under the curve shortening flow. We can use the parabolic structure of some of the differential equations to extend this result. We also use these equations to derive the evolution of global quantities related to the curve, such as its arc length. In some cases the differential equations also have steady state solutions or their order can be reduced by applying symmetry methods. Similar results are collected in [16].

3.2.1 No new vertices

According to Angenent the number of vertices of a curve flowing under the curve shortening flow is non-increasing in time. We can replicate this result by studying

the evolution of signatures and extend it by finding other flows where the same property holds. Here we state our theorem for a class of signature flows, and later we will apply this to specific cases.

Theorem 3.2 *Let $C(t), 0 \leq t \leq T$ be a time-dependent family of regular curves. Let $\kappa_s = H(\kappa, t)$ be the corresponding local signature function that evolves according to the partial differential equation*

$$H_t = F_2(\kappa, H)H_{\kappa\kappa} + F_1(\kappa, H)H_\kappa + F_0(\kappa, H)H. \tag{3.5}$$

If

$$F_2(\kappa, H) \geq 0, \qquad F_0(\kappa, H) \geq 0$$

and if $H \in \mathcal{C}^{2,1}(\Gamma)$, then the number of vertices of the curve is a non-increasing function of time.

Proof We consider the case that H begins positive on the interior of its domain. We want to show that H does not become zero on the interior of the domain as it evolves. Since the partial differential equation becomes degenerate at the endpoints we cut out an arbitrarily small portion near each endpoint. First we pick a $\delta > 0$ such that $\Gamma_0^\delta = \{(\kappa, 0) | H(\kappa, 0) > \delta\}$ is a nonempty connected set. Let $a^\delta(0), b^\delta(0)$ be the left and right endpoints of Γ_0^δ. The evolution of these endpoints is given by equation (3.4). Let

$$\Gamma^\delta(T^\delta) = \{(\kappa, t) | a^\delta(t) \leq \kappa \leq b^\delta(t), 0 \leq t \leq T^\delta\}$$

and

$$\partial\Gamma^\delta = \big([a^\delta(0), b^\delta(0)] \times \{t = 0\}\big) \cup \{(a^\delta(t), t) | 0 \leq t \leq T^\delta\} \cup \{(b^\delta(t), t) | 0 \leq t \leq T^\delta\}$$

be the parabolic boundary of Γ^δ. The parameter T^δ depends on δ, it is the minimum value of t for which $H_\kappa(a^\delta(t), t) = 0$, $H_\kappa(b^\delta(t), t) = 0$. We consider the function $v(\kappa, t) = \dfrac{1}{H} - \epsilon t$ for some arbitrarily small $\epsilon > 0$. Since $H \geq \delta$ on $\partial\Gamma^\delta$

we have $v \leq \frac{1}{\delta}$ on $\partial\Gamma^\delta$. The function v solves the partial differential equation

$$\begin{aligned} v_t =& F_2\left(\kappa, \frac{1}{v+\epsilon t}\right) v_{\kappa\kappa} - F_2\left(\kappa, \frac{1}{v+\epsilon t}\right)\frac{v_\kappa^2}{v} + F_1\left(\kappa, \frac{1}{v+\epsilon t}\right) v_\kappa \\ & - F_0\left(\kappa, \frac{1}{v+\epsilon t}\right) v - \epsilon. \end{aligned} \tag{3.6}$$

Suppose that v_t obtains a maximum on the interior of Γ^δ or at $t = T^\delta$. At this point we have

$$v_t \geq 0 \quad F_2\, v_{\kappa\kappa} \leq 0 \quad v_\kappa = 0 \quad -F_0\, v \leq 0.$$

This contradicts (3.6) so $\max\limits_{\Gamma^\delta}(v) = \max\limits_{\partial\Gamma^\delta}(v)$. Letting ϵ go to zero implies $\min\limits_{\Gamma^\delta} H = \min\limits_{\partial\Gamma^\delta}(H) = \delta$. Since δ is arbitrary we can let it go to 0. Since H_κ is unbounded as we approach the endpoints $(a(t), b(t))$, as discussed in section 3.1, we have $\lim_{\delta\to 0+} T^\delta = T$, so we obtain the result for $H > 0$. A proof for the case where $H \leq 0$ follows the same pattern.

3.3 Euclidean signature evolutions

3.3.1 Curve shortening flow

First we consider the evolution of the differential invariant signature under the curve shortening flow, where the curve moves under the normal velocity $J = \kappa$. We find a few solutions to these equations, we reconfirm Theorem 3.2, and we show how these evolution equations can be used to find the evolution of global geometric quantities.

First we note that the evolutionary partial differential equation for the signature under the curve shortening flow, equation (3.3), meets all the conditions of Theorem 3.2. Thus we reconfirm Angenent's [4] result on the non-increase in the number of vertices for this flow.

Special solutions of the curve shortening flow

Now we look for particular solutions to (3.3). First we will ignore the time variable and look for equilibrium solutions of the following ODE

$$H^2 H_{\kappa\kappa} - \kappa^3 H_\kappa + 4\kappa^2 H = 0. \tag{3.7}$$

This second order ODE has an integrating factor $\mu = \dfrac{\kappa}{H(\kappa)^2}$, so

$$\mu\left(H^2 H_{\kappa\kappa} - \kappa^3 H_\kappa + 4\kappa^2 H\right) = \frac{d}{d\kappa}\left(\kappa H_\kappa + \frac{\kappa^4 - H^2}{H} + C\right).$$

This simplifies ODE to

$$\kappa H_\kappa + \frac{\kappa^4 - H^2}{H} + C = 0$$

where C is an arbitrary constant. If we set $C = 0$ then we have a family of solutions parameterized by b,

$$H(\kappa) = \pm\kappa\sqrt{b^2 - \kappa^2}. \tag{3.8}$$

This signature corresponds to the "grim reaper" curves

$$u(x) = \frac{\log(\sec bx)}{b} + C, \quad x \in \left(\frac{-\pi}{2b}, \frac{\pi}{2b}\right). \tag{3.9}$$

To see that (3.8) is a solution to (3.7) we recall the formula for Euclidean curvature and invariant differential operator given in 2.4.1. If we assume that $0 < x < \frac{\pi}{2b}$, we find

$$\kappa = \frac{1}{b\sqrt{\sec^2 \dfrac{x}{b}}} = b\cos bx \qquad \kappa_s = \frac{-b^2 \sin 2bx}{2}.$$

Returning to equation 3.8

$$\kappa\sqrt{b^2 - \kappa^2} = b\cos bx\sqrt{b^2 - b^2\cos^2 bx} = b^2\cos bx,\ \sin bx = -\frac{1}{2}b^2 \sin 2bx = \kappa_s,$$

we see that Equation (3.7) also has a scaling symmetry

$$\tilde{\kappa} = \lambda\kappa, \quad \tilde{H} = \lambda^2 H,$$

which corresponds to the infinitesimal generator

$$\mathbf{v} = \kappa\,\partial\kappa + 2H\,\partial H.$$

To find rectifying coordinates we need to solve the differential equations $\mathbf{v}(y) = 0$, $\mathbf{v}(w) = 1$. The functions $y(\kappa, H) = \dfrac{H}{\kappa^2}, w(\kappa, H) = \ln(\kappa)$ work. The differential equation becomes a first order differential equation for the function $F(y) = \dfrac{dw}{dy}$. Using these coordinates we make the change of variables

$$y = \frac{H(\kappa)}{\kappa^2}, \qquad F(y) = \frac{\kappa^2}{H_\kappa \kappa - 2H(\kappa)}$$

$$H(\kappa) = \exp\left(2\int F(y)dy + 2c\right)y, \qquad \kappa = \exp\left(\int F(y)dy + c\right),$$

and obtain a new differential equation for the function $F(y)$

$$\frac{d}{dy}F(y) = \frac{2y(y^2+1)F(y)^3 + (-1+3y^2)F(y)^2}{y^2}, \tag{3.10}$$

which is an Abel equation of the second kind. These types of equations generally do not have solutions that can be represented with elementary functions.

Similarity solutions

Looking at the PDE (3.3) we see that this equation also has a scaling symmetry. The infinitesimal generator is $-\frac{1}{2}\,\kappa\partial_\kappa + t\partial_t - H\partial_H$. The rectifying coordinates

$$F(y) = \frac{H(\kappa, t)}{\kappa^2}, \quad y = t\kappa^2, \quad z = t$$

eliminate the dependence on the variable z. The inverse transformation is given by

$$H(\kappa, t) = \frac{yF(y, z)}{z}, \quad \kappa = \sqrt{\frac{y}{z}}, \quad t = z.$$

Using Maple, we find the transformation of (3.3) is

$$-\frac{y^2\left(-F_y + 2F^3 + 10yF^2F_y + 4y^2F^2F_{yy} + 2F - 2yF_y\right)}{s^2} = 0 \tag{3.11}$$

$$4y^2F^2F_{yy} + \left(10yF^2 - 2y - 1\right)F_y + 2\left(F + F^3\right) = 0. \tag{3.12}$$

Equation (3.11) has an integrating factor

$$\mu = \frac{1}{F^2 y^2}$$

which further reduces the equation to

$$\frac{1}{2}yF + \frac{2y+1}{4F} + y^2 F_y + C = 0. \tag{3.13}$$

Setting $C = 0$, we find the solution

$$F(y) = \pm\frac{\sqrt{-2y\,(2y + \ln(y) - 2C)}}{2y}.$$

Mapping back to the original coordinates we find

$$H(\kappa, t) = \pm\frac{\sqrt{-2t\kappa^2(2t\kappa^2 + \ln(t\kappa^2) - 2C)}}{2t} = \pm\frac{\kappa}{t^{1/2}}\sqrt{C - t\kappa^2 - \ln(\kappa t^{1/2})}. \tag{3.14}$$

The curves corresponding to these signatures do not seem to have a simple, closed form solution, unlike the grim-reaper curves. We have approximated a few of these curves by solving (3.14) numerically for $C = 1, t = 1$. We start with the initial conditions $y(0) = y'(0) = 0, y''(0) = 1$ so that $\kappa = 1$, the maximum curvature, at the origin. The curve turns up in both directions, so $y(x) \geq 0$. It also appears to not be a closed curve and it appears to be infinitely long as κ approaches 0.

Evolution of global geometric measures

A number of geometric features can be expressed as an integral of some function taken with respect to the arc length. We can study the evolution of these quantities by changing the parameterization from the arc length to κ. The signature function $H = \kappa_s$ gives us the derivative of the mapping between the parameterizations. Away from $\kappa_s = 0$ this leads to the change of variables for the integral

$$\int ds = \int \frac{1}{H} H ds = \int \frac{1}{H(\kappa, t)} d\kappa. \tag{3.15}$$

We can study how this evolves by differentiating the integral with respect to time. This becomes troublesome as H approaches 0. As in section 3.1.1, we define

functions $a^\delta(t), b^\delta(t)$ such that $H(a^\delta(t),t) = H(b^\delta(t) = \delta$, and then we let δ go to 0.

Using this information we can take the derivative with respect to time

$$\begin{aligned}
\frac{d}{dt}\int_{a^\delta(t)}^{b^\delta(t)} \frac{1}{H(\kappa,t)}d\kappa &= -\frac{H_t}{HH_\kappa}\Big|_{a^\delta}^{b^\delta} - \int_{a^\delta}^{b^\delta}\frac{H_t}{H^2}d\kappa \\
&= -\frac{H^2H_{\kappa\kappa} - \kappa^3H_\kappa + 4\kappa^2H}{HH_\kappa}\Big|_{a^\delta}^{b^\delta} - \int_{a^\delta}^{b^\delta}\left(H_{\kappa\kappa} - \frac{\kappa^3H_\kappa}{H^2} + \frac{4\kappa^2}{H}\right)d\kappa \\
&= -\frac{H^2H_{\kappa\kappa} - \kappa^3H_\kappa + 4\kappa^2H}{HH_\kappa} - H_\kappa\Big|_{a^\delta}^{b^\delta} - \int_{a^\delta}^{b^\delta}\left(\frac{d}{d\kappa}\left(\frac{\kappa^3}{H}\right) + \frac{\kappa^2}{H}\right)d\kappa \\
&= -\frac{H^2H_{\kappa\kappa} + 4\kappa^2H}{HH_\kappa} - H_\kappa\Big|_{a^\delta}^{b^\delta} - \int_{a^\delta}^{b^\delta}\frac{\kappa^2}{H}d\kappa \\
&= -\frac{H^2H_{\kappa\kappa} + HH_\kappa^2 + 4\kappa^2H}{HH_\kappa}\Big|_{a^\delta}^{b^\delta} - \int_{a^\delta}^{b^\delta}\frac{\kappa^2}{H}d\kappa.
\end{aligned}$$

As $\epsilon \to 0$, the term $\dfrac{4\kappa^2H}{HH_\kappa} = \dfrac{4\kappa^2}{H_\kappa} = 0$, since $H_\kappa \to \infty$, due to Theorem 3.1. Recalling equation 3.1, the remaining part of the boundary term - $\dfrac{H^2H_{\kappa\kappa} + HH_\kappa^2}{HH_\kappa}$ is exactly -$\dfrac{\kappa_{sss}}{\kappa_{ss}}$. As long as $\kappa_{ss} \neq 0$ at the endpoint, which is true as long as the evolving curve remains regular, the boundary terms will be finite. When we integrate over an entire curve the same boundary terms will appear on one of the adjacent segments of the curve, but with an opposite sign. Across an entire closed curve the boundary terms will cancel each other out. This leads to the following evolution for the arc length

$$\frac{d}{dt}\int ds = -\int\frac{\kappa^2}{H}d\kappa = -\int\kappa^2 ds.$$

Invariant signatures can be used to study the evolution of other geometric quantities. Here we will look at

$$\frac{d}{dt}\int\kappa^\alpha ds = \frac{d}{dt}\int\frac{\kappa^\alpha}{H}d\kappa.$$

We integrate by parts, and ignore the boundary terms since they will cancel out

when we integrate over a closed curve.

$$\begin{aligned}
&\frac{d}{dt}\int \frac{\kappa^\alpha}{H} d\kappa = -\int \frac{\kappa^\alpha H_t}{H^2} d\kappa \\
&= -\int \left(\kappa^\alpha H_{\kappa\kappa} - \frac{\kappa^{3+\alpha} H_\kappa}{H^2} + \frac{4\kappa^{2+\alpha}}{H} \right) d\kappa \\
&= -\int \left(-\alpha\kappa^{\alpha-1} H_\kappa - \frac{\kappa^{3+\alpha} H_\kappa}{H^2} + \frac{4\kappa^{2+\alpha}}{H} \right) d\kappa \\
&= -\int \left(\alpha(\alpha-1)\kappa^{\alpha-2} H - \frac{\kappa^{3+\alpha} H_\kappa}{H^2} + \frac{4\kappa^{2+\alpha}}{H} \right) d\kappa \\
&= -\int \left(\alpha(\alpha-1)\kappa^{\alpha-2} H + \frac{d}{d\kappa}\frac{\kappa^{3+\alpha}}{H} + (1-\alpha)\frac{\kappa^{2+\alpha}}{H} \right) d\kappa \\
&= -\int \left(\alpha(\alpha-1)\kappa^{\alpha-2} H + (1-\alpha)\frac{\kappa^{2+\alpha}}{H} \right) d\kappa \\
&= -\int \left(\alpha(\alpha-1)\kappa^{\alpha-2}\kappa_s^2 + (1-\alpha)\kappa^{2+\alpha} \right) ds.
\end{aligned}$$

One interesting case is $\alpha = 1$, where $\int \kappa ds = 2\pi$ for a closed, embedded curve. Both parts of the integral are 0, so $\frac{d}{dt}\int \kappa\, ds = 0$, as expected.

3.3.2 Other Euclidean curvature motions

Previously we have assumed that we have a curve that is moving under the curve shortening flow, namely it moves in the normal direction with speed $J = \kappa$. Now we move the curve with velocity $J = \kappa^\alpha$, and we find the partial differential equation which the signature must solve. We have the following differential operators which were derived in section 2.5

$$A_\kappa = \mathcal{D}^2 + \kappa^2, \qquad A_{\kappa_s} = \mathcal{D}^3 + \kappa^2\mathcal{D} + 3\kappa\kappa_s,$$

which we apply to J to find $\dfrac{\partial\kappa}{\partial t}, \dfrac{\partial\kappa_s}{\partial t}$. We also have

$$\begin{aligned}
\mathcal{D}\kappa^\alpha =&\alpha\kappa^{\alpha-1}\kappa_s = \alpha\kappa^{\alpha-1}H\\
\mathcal{D}^2\kappa^\alpha =&\alpha(\alpha-1)\kappa^{\alpha-2}\kappa_s^2 + \alpha\kappa^{\alpha-1}\kappa_{ss} = \alpha(\alpha-1)\kappa^{\alpha-2}H^2 + \alpha\kappa^{\alpha-1}HH_\kappa\\
\mathcal{D}^3\kappa^\alpha =&\alpha(\alpha-1)(\alpha-2)\kappa^{\alpha-3}\kappa_s^3 + 3\alpha(\alpha-1)\kappa^{\alpha-2}\kappa_s\kappa_{ss} + \alpha\kappa^{\alpha-1}\kappa_{sss}\\
=&\alpha(\alpha-1)(\alpha-2)\kappa^{\alpha-3}H^3 + 3\alpha(\alpha-1)\kappa^{\alpha-2}H^2H_\kappa\\
&+\alpha\kappa^{\alpha-1}(H^2H_{\kappa\kappa} + HH_\kappa^2).
\end{aligned}$$

The evolutionary equation for the signature is:

$$\begin{aligned}
H_t =&H^2H_{\kappa\kappa}\alpha\kappa^{\alpha-1} + H_\kappa(2\alpha(\alpha-1)\kappa^{\alpha-2}H^2 - \kappa^{2+\alpha})\\
&+\alpha(\alpha-1)(\alpha-2)\kappa^{\alpha-3}H^3 + (\alpha+3)\kappa^{\alpha+1}H.
\end{aligned} \tag{3.16}$$

Equation (3.16) can be written in the form of (3.6) as

$$\begin{aligned}
H_t =&H^2H_{\kappa\kappa}\alpha\kappa^{\alpha-1} + H_\kappa(2\alpha(\alpha-1)\kappa^{\alpha-2}H^2 - \kappa^{2+\alpha})\\
&+\left(\alpha(\alpha-1)(\alpha-2)\kappa^{\alpha-3}H^2 + (\alpha+3)\kappa^{\alpha+1}\right)H.
\end{aligned}$$

If $J = J(\kappa)$ is an arbitrary function of κ we have

$$\begin{aligned}
\frac{\partial\kappa}{\partial t} &= J''\kappa_s^2 + J'\kappa_{ss} + J\kappa^2 = J''H^2 + J'HH_\kappa + J\kappa^2\\
\frac{\partial\kappa_s}{\partial t} &= J'''\kappa_s^3 + 3J''\kappa_s\kappa_{ss} + J'\kappa_{sss} + J'\kappa^2\kappa_s + 3J\kappa\kappa_s\\
\frac{\partial\kappa_s}{\partial t} &= J'''H^3 + 3J''H^2H_\kappa + J'(HH_\kappa^2 + H^2H_{\kappa\kappa}) + J'H\kappa^2 + 3JH\kappa
\end{aligned}$$

$$\begin{aligned}
H_t &= J'H^2H_{\kappa\kappa} + J'''H^3 + 2J''H^2H_\kappa + J'H\kappa^2 + 3JH\kappa - JH_\kappa\kappa^2\\
H_t &= J'H^2H_{\kappa\kappa} + \left(2J''H^2 - J\kappa^2\right)H_\kappa + (J'''H^2 + J'\kappa^2 + 3J\kappa)H.
\end{aligned} \tag{3.17}$$

No new vertices

If we have a strictly convex curve, $\kappa > 0$, we can see that the curve cannot develop any new vertices for $0 < \alpha \leq 1$, or $\alpha \geq 2$.

Corollary 3.3 *Let $C(t)$ be a curve evolving under the normal motion given by $J = \kappa^\alpha$ for $0 \leq \alpha \leq 1$, or $\alpha \geq 2$. Let T be the maximum time for which $C(t), 0 \leq t < T$ is strictly convex and regular. The number of vertices of $C(t)$ is non-increasing for $0 \leq t \leq T$.*

This includes the case $J = \kappa^{\frac{1}{3}}$ which is equivalent to the equi-affine invariant flow [5]. This property may not hold in the case where $1 < \alpha < 2$ since the term

$$\alpha(\alpha-1)(\alpha-2)\kappa^{\alpha-3}H^3$$

has the opposite sign as H and this can lead to our signature crossing the κ axis. We need the condition that $C(t)$ is strictly convex since the term $\kappa^{\alpha-3}$ appears in equation (3.17), which is not well defined if $\alpha < 3$ and $\kappa = 0$ anywhere.

Proof To use Theorem 3.2 we must show that

$$\alpha\kappa^{\alpha-1}H^2 \geq 0$$

$$\alpha(\alpha-1)(\alpha-2)\kappa^{\alpha-3}H^2 + (\alpha+3)\kappa^{\alpha+1} \geq 0.$$

Both of these inequalities hold if $0 \leq \alpha \leq 1,$ or $\alpha \geq 2$ and $\kappa > 0$.

Under the more general curve flow given by $J = J(\kappa)$, the conditions of Theorem 3.2 hold if

$$\kappa > 0, \quad J\kappa \geq 0, \quad J' \geq 0, \quad J''' \geq 0.$$

Evolution of geometric quantities

As in section 3.3.1 we can also derive the evolution of the arc length from the above PDE for the signature

$$\begin{aligned}
\frac{d}{dt}\int ds = \frac{d}{dt}\int \frac{1}{H}d\kappa &= -\int \frac{H_t}{H^2}d\kappa \\
&= -\int J'H_{\kappa\kappa} + J'''H + 2J''H_\kappa + \frac{J'\kappa^2 + 3J\kappa}{H} - \frac{JH_\kappa\kappa^2}{H^2}d\kappa \\
&= -\int 2J'H - 2J'H + \frac{d}{d\kappa}\frac{J\kappa^2}{H} + \frac{J\kappa}{H}d\kappa \\
&= -\int J\kappa ds.
\end{aligned}$$

This result agrees with calculations in [16]. Finding expressions for the evolution of any other quantity that we are interested in is straightforward.

3.3.3 Area preserving curvature motion

The curve shortening flow seems to do a good job of eliminating small differences between curves, but it also only exists for a finite time. A number of different methods have been suggested for altering this flow so that the resulting flow preserves the area [23],[28],[20]. One way to modify the flow to make it area preserving by subtracting the mean of the curvature

$$J = \kappa - \overline{\kappa}, \qquad \overline{\kappa} = \frac{\int \kappa ds}{\int ds}.$$

The evolution of κ and κ_s are given by

$$\begin{aligned} \frac{\partial \kappa}{\partial t} &= \kappa_{ss} + \kappa^3 - \kappa^2 \overline{\kappa}, \\ \frac{\partial \kappa_s}{\partial t} &= \kappa_{sss} + 4\kappa^2 \kappa_s - 3\kappa \kappa_s \overline{\kappa}. \end{aligned}$$

The partial differential equation that the signature solves is

$$H_t = H^2 H_{\kappa\kappa} - \kappa^3 H_\kappa + 4\kappa^2 H + \overline{\kappa}(\kappa^2 H_\kappa - 3\kappa H).$$

The quantity $\overline{\kappa}$ is a non-local term so this can be seen as an integro-differential equation.

Evolution of geometric quantities

This partial differential equation can be used to study the evolution of other geometric quantities of the curve, such as

$$\begin{aligned}\frac{d}{dt}\int \kappa^\alpha ds &= \frac{d}{dt}\int \frac{\kappa^\alpha}{H} d\kappa = -\int \frac{\kappa^\alpha H_t}{H^2} d\kappa \\ &= -\int \left(\kappa^\alpha H_{\kappa\kappa} - \frac{\kappa^{3+\alpha} H_\kappa}{H^2} + \frac{4\kappa^{2+\alpha}}{H} + \overline{\kappa}\left(\frac{\kappa^{2+\alpha} H_\kappa}{H^2} - \frac{3\kappa^{1+\alpha}}{H}\right)\right) d\kappa \\ &= -\int \left(\alpha(\alpha-1)\kappa^{\alpha-2} + \frac{(1-\alpha)\kappa^{2+\alpha}}{H} - \overline{\kappa}\left((1-\alpha)\frac{\kappa^{1+\alpha}}{H}\right)\right) d\kappa \\ &= -\int \left(\alpha(\alpha-1)\kappa^{\alpha-2}\kappa_s + (1-\alpha)\kappa^{2+\alpha} - \overline{\kappa}(1-\alpha)\kappa^{1+\alpha}\right) ds.\end{aligned}$$

Some cases that are particularly interesting are $\alpha = 0$, where the integral gives the length of the curve, and $\alpha = 1$ where the integral should be equal to 2π when the curve is closed, smooth, and embedded. For the case $\alpha = 0$ the equation simplifies to

$$\frac{d}{dt}\int \frac{1}{H} d\kappa = \int -\frac{\kappa^2}{H} + \overline{\kappa}\frac{\kappa}{H} d\kappa = \int -\kappa^2 ds + \frac{(\int \kappa ds)^2}{\int ds},$$

and this can be used to find a differential equation for $\overline{\kappa}$

$$\frac{d}{dt}\overline{\kappa} = \frac{d}{dt}\frac{\int \kappa ds}{\int ds} = \frac{-2\pi L_t}{L} = -2\pi \frac{L\int -\kappa^2 ds + \left(\int \kappa ds\right)^2}{L^2} = 2\pi(\overline{\kappa^2} - \overline{\kappa}^2).$$

This is 2π times the variance of of κ with respect to the arc length. It's a non negative quantity, so $\bar{\kappa}$ is a nondecreasing function with respect to time. If the curve is closed then this also means that the length of the curve is non-increasing, $L_t \leq 0$.

When $\alpha = 1$ we find that each remaining term in the integral is multiplied by 0 so we can,as expected, conclude

$$\frac{d}{dt}\int \kappa ds = 0$$

since $\int \kappa ds = 2\pi$, as long as the curve is closed and embedded.

There are examples where curves evolving under this flow develop singularities [36]. To avoid singularities we can scale the curve as it evolves to maintain the area as in [53]. Taking this approach we find an evolution which is local, but it depends on quantities that are not local Euclidean invariants.

3.4 Evolution of invariants under other group actions

3.4.1 Equi-affine group

Here we examine the equi-affine signature evolution when the curve flows under the normal motion with a velocity of $J = 1$. The necessary Eulerian operators are found in section 2.4.4

$$\begin{aligned}
\frac{\partial \kappa}{\partial t} &= \mathcal{A}_\kappa(1) = \frac{\kappa_{ss}}{3} + \frac{4}{9}\kappa^2 \\
\frac{\partial \kappa_s}{\partial t} &= \mathcal{A}_{\kappa_s}(1) = \frac{\kappa_{sss}}{3} + \frac{10}{9}\kappa_s\kappa \\
H_t &= \frac{\kappa_{sss}}{3} + \frac{10}{9}\kappa_s\kappa - \frac{H_\kappa}{3}\kappa_{ss} - \frac{4H_\kappa}{9}\kappa^2 \\
H_t &= \frac{H_{\kappa\kappa}H^2 + H_\kappa^2 H}{3} + \frac{10}{9}H\kappa - \frac{H_\kappa}{3}H_\kappa H - \frac{4H_\kappa}{9}\kappa^2 \\
H_t &= \frac{1}{9}\left(3H_{\kappa\kappa}H^2 - 4\kappa^2 H_\kappa + 10\kappa H\right). \qquad (3.18)
\end{aligned}$$

This is a parabolic equation which degenerates as H approaches 0.

Similarity solutions

Now that we have a PDE describing the evolution of the signature function, what can we learn from this PDE? We begin by looking for steady state solutions by setting $H_t = 0$ and studying the ODE

$$3H_{\kappa\kappa}H^2 - 4H_\kappa\kappa^2 + 10H\kappa = 0. \qquad (3.19)$$

This equation has a symmetry generator

$$\kappa\partial_\kappa + \frac{3}{2}H\partial_H$$

with the rectifying coordinates

$$y = \frac{H}{\kappa^{3/2}}, \quad w = \ln(\kappa), \quad F(y) = \frac{dw}{dy},$$

which give the change of variables

$$\kappa = \exp\left(\int F(y)dy + C\right), \quad H = \exp\left(\frac{3}{2}\left(\int F(y)dy + C\right)\right) y.$$

This simplifies (3.19) to

$$F_y = \frac{(9y^2+16)F^3 + 8y(3y^2-2)F^2}{12y^2}.$$

Unlike (3.7) this ODE does not appear to have an integrating factor.

Returning to the symmetry group of the full PDE (3.18) has two generators

$$\partial_t, \quad -\kappa\partial_\kappa + t\partial_t - \frac{3}{2}H\partial_H.$$

The first symmetry generator eliminates the time variable, and leads us to (3.19). Using the second generator we try the change of variables

$$t = z, \quad H(\kappa, t) = F(y)\left(\frac{y}{z}\right)^{3/2}, \quad \kappa = \frac{y}{z},$$

which reduces (3.18) to the second order ODE

$$36F_y = 12F^2y^2F_{yy} + 36F^2yF_y + 9F^3 - 16yF_y + 16F. \tag{3.20}$$

No new vertices

A Euclidean vertex is any point on a curve which is a local extrema of the Euclidean curvature. Likewise an *equi-affine vertex* is a local minimum or maximum of the equi-affine curvature, equation (2.33). A curve is strictly *equi-affine convex* if the equi-affine curvature $\kappa > 0$. The parabolic structure of (3.18) lets us extend the theorem on the non-increase in the number of vertices to the equi-affine flow with $J = 1$ if the curve is strictly equi-affine convex.

Corollary 3.4 *Let $C(t)$ be a family of regular, equi-affine convex curves evolving under the equi-affine invariant motion with normal velocity $J = 1$. The number of vertices is a non-increasing function of time.*

Proof If the curve is equi-affine convex, then $\kappa > 0$. Under the normal velocity $J = 1$ the signature evolution (3.18) meets all the criteria of Theorem 3.2.

3.4.2 Similarity group

Here we look at the signature evolution under the similarity group for $J = 1$. We stick to this case since the resulting PDE is second order. Using the Eulerian operators found in section 2.4.5 we obtain the evolution of the differential invariants

$$\frac{\partial \kappa}{\partial t} = -\kappa_{ss} + \kappa\kappa_s$$
$$\frac{\partial \kappa_s}{\partial t} = -\kappa_{sss} + \kappa_{ss}\kappa + 2\kappa_s^2.$$

The signature function $\kappa_s = H(\kappa, t)$ evolves according to the PDE

$$H_t = -H_{\kappa\kappa}H^2 + 2H^2.$$

Similarity solutions

This PDE has three different symmetry generators

$$\partial_t, \quad \partial_\kappa, \quad -\frac{1}{2}\kappa\partial_\kappa + t\partial_t - H\partial_H.$$

Using these symmetries leads to a few particular solutions

$$H_1(\kappa, t) = \frac{1}{-2t + C},$$
$$H_2(\kappa, t) = \kappa^2 + C_1\kappa + C_2.$$

The curves related to H_1 all have κ_s as a constant for each time. They exist up to $t = C/2$. The curves related to H_2 are completely invariant under the flow, like the grim-reaper curves of the Euclidean group. There are solutions for the curves related to these signatures. The exact formulas are omitted.

Using the third symmetry generator we try the change of variables

$$H(\kappa, t) = \frac{yF(y)}{t}, \quad \kappa = \sqrt{\frac{y}{t}},$$

which eliminates the t variable and reduces the equation to

$$y^2F_y = -2y^2\,F^2\left(F + 5yF_y + 2y^2F_{yy} - 2\right).$$

This ODE has exact solutions involving the Kummer functions as defined in [1]. Alternatively this ODE has an integrating factor y^2 which further reduces the ODE to

$$\frac{4y^2FF_y - 1 + 2yF^2 - 2yF}{F} + C_1 = 0.$$

If we set $C_1 = 0$ we get an Abel equation of second type, class B, which has the implicit solution

$$C_2 + \frac{\sqrt{-2y\pi}\ \mathrm{erf}(\sqrt{-y}(-1+F(y))) - \sqrt{2}\exp(y(-1+F(y))^2)}{\sqrt{-y}} = 0$$

where erf is the error function which is defined as

$$\mathrm{erf}(x) = \frac{2}{\sqrt{\pi}}\int_0^x e^{-t^2}dt.$$

3.4.3 Centro-affine signatures, special solutions

When we study the centro-affine group acting on space curves we found the differential invariants κ,τ,κ_s. The first differential invariant κ is of order 3 and the others are of order 4. If the rank of the map from the curve C to κ is 1 on the entire curve then the differential invariant signature is the set $\{(\kappa(z), \tau(z), \kappa_s(z), |z \in C\}$. We assume that this signature can be represented by the functions

$$\tau = \psi(\kappa, t), \qquad \kappa_s = \phi(\kappa, t).$$

Under the evolution given by $J^1 = 0, J^2 = 1$ the evolution of the differential invariants is

$$\frac{\partial\kappa}{\partial t} = -3\kappa, \frac{\partial\tau}{\partial t} = -2\tau, \frac{\partial\kappa_s}{\partial t} = -4\kappa_s,$$

which leads to the following partial differential equations for ϕ, ψ

$$\frac{\partial\phi}{\partial t} = 3\phi_\kappa - 4\phi, \frac{\partial\psi}{\partial t} = 3\psi_\kappa - 2\psi.$$

These equations have the general solution

$$\phi(\kappa, t) = F_1\left(t + \frac{1}{3}\ln\kappa\right)\kappa^{4/3}$$

$$\psi(\kappa, t) = F_2\left(t + \frac{1}{3}\ln\kappa\right)\kappa^{2/3}$$

where F_1, F_2 are arbitrary functions.

3.5 Similarity group invariants in terms of Euclidean invariants

There is also a connection between the differential invariants of the similarity group and the Euclidean invariants. Since the Euclidean group is a subgroup of the similarity group, the relationships between differential invariants for these different groups can be found using Kogan's inductive construction of moving frames [30]. Here we let $\varkappa = I_3$ be the first differential invariant under the similarity group and we let $\kappa, \kappa_s, ...$ be the differential invariants of the Euclidean group. With the normalizations that we have chosen we have $\varkappa = \frac{\kappa_s}{\kappa^2}$. Higher order invariants of the similarity group can be found using the similarity invariant differential operator $\mathcal{D} = \frac{1}{\kappa}D_s$, where D_s is the invariant differential operator for the Euclidean group.

Suppose we take the motion with $\tilde{I} = 1$ in the scale invariant case. We find that the evolution of $\varkappa$ is given by

$$A_{\varkappa}(1) = -\varkappa_{ss} + \varkappa\varkappa_s = \frac{8\kappa_{ss}\kappa_s\kappa - 10\kappa_s^3 + \kappa_{sss}\kappa^2}{\kappa^6}.$$

The unit normal vector for the scaling group is

$$\tilde{\mathbf{n}} = \frac{1 + u_x^2}{u_{xx}}\left(-u_x\frac{\partial}{\partial x} + \frac{\partial}{\partial u}\right).$$

The unit normal for the Euclidean group is

$$\mathbf{n} = \frac{1}{\sqrt{1 + u_x^2}}\left(-u_x\frac{\partial}{\partial x} + \frac{\partial}{\partial u}\right)$$

so we have $\tilde{\mathbf{n}} = \frac{1}{\kappa}\mathbf{n}$. Therefore, if we wish to match a motion with $\tilde{I} = 1$ in the scaling group we should take a motion in the Euclidean group with $J = \frac{1}{\kappa}$. Now

we find the evolution of $\frac{\kappa_s}{\kappa^2}$

$$d_v\left(\frac{\kappa_s}{\kappa^2}\right) = \left(-\frac{2\kappa_s D^2}{\kappa^3} + \frac{\kappa_s}{\kappa} + \frac{D^3}{\kappa^2} + D\right)\vartheta_0$$

$$\mathcal{A}_{\frac{\kappa_s}{\kappa^2}} = \left(-\frac{2\kappa_s D^2}{\kappa^3} + \frac{\kappa_s}{\kappa} + \frac{D^3}{\kappa^2} + D\right)$$

$$\mathcal{A}_{\frac{\kappa_s}{\kappa^2}}\left(\frac{1}{\kappa}\right) = \frac{8\kappa_{ss}\kappa_s\kappa - 10\kappa_s^3 + \kappa_{sss}\kappa^2}{\kappa^6}.$$

Chapter 4

Curve classification

In this chapter we describe an experiment in classifying curves. We start by describing a set of curves that we have extracted from a computer vision segmentation dataset and a method for using differential invariant signatures and the curve shortening flow to build a curve classifier from the dataset. The training and cross-validation was done using the Multivariate Pattern Analysis in Python toolbox (PyMVPA) [27].

4.1 Dataset

We started from the Berkeley Segmentation Dataset [35] which is a collection of 300 images, each hand segmented by 10 to 15 different subjects. Each segmentation is given as a number of regions. Some of the images are cluttered and full of many different objects, so we first discarded any segmentations with more then 15 different regions. For any remaining segmentations we searched for regions whose boundaries were closed curves and at least 600 pixels long. If the segmented region had more then one boundary we took the longest of the boundaries. Generally this would be the outside boundary. If regions R^1, R^2 from two different segmentations of the same image had a large overlap, specifically

$$area(R^1 \cap R^2) > .6\, max(area(R^1), area(R^2)),$$

then it is likely that the two regions represent the same object from the image and we give the boundaries of these two regions the same label. After this we take any label with five or more curves. All of the other curves are discarded. This process leads to a labeled database of 350 curves with 33 different labels. For example consider the images of the wolf and the palm tree in figure 4.1. Most of the segmentations of these images largely agreed on the region that corresponds to the wolf and the palm tree. All of the boundaries of the different segmentations of the wolf will be given the same label, and all of the boundaries of the different segmentations of the palm tree will be given the same label.

(a) An image of a wolf.

(b) An image of a palm tree.

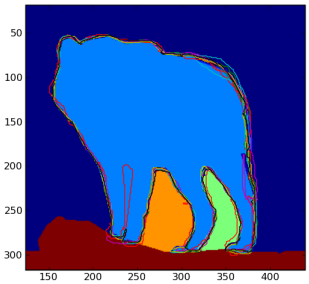

(c) One segmentation of the wolf image along with the boundaries of the wolf from different segmentations

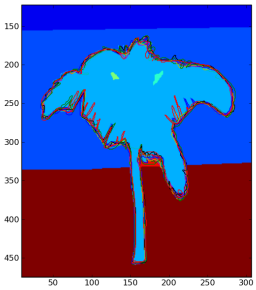

(d) One segmentation of the palm tree along with the boundaries of the palm tree from different segmentations

Figure 4.1: These are examples of two images, with the curves in the lower images representing the boundaries of different segmentations.

4.1.1 Occlusion and smoothing

Two main obstacles to classifying curves are occlusion and the different amount of detail in the different segmentations of the same object. We see both of these problems in the segmentations of the palm tree. Most of the subjects labeled the trunk and the leaves as the same region but one subject decided that the trunk should be a separate region from the leaves. This is an example of occlusion. The boundary of the trunk is missing from the curve for this one curve. Since differential invariants are local functions the only missing information is from the trunk. The differential invariants related to the leaves should still have the same information as the invariants from the other palm trees.

Along with these large scale differences the curves produced from the boundaries of these regions also differ in the amount of detail. Some subjects included a high amount of detail in the leaves of the tree while others made regions that gave smoother curves. To reduce the differences we propose using the curve shortening flow. Under the curve shortening flow small, high frequency details are eroded faster than larger, low frequency details. If we begin with two curves where one is a more detailed version of another, then after a certain amount of time, their smoothed versions should resemble each other. Although this happens in practice, as we show with our dataset, we do not have a theorem to this effect.

The curves that we have extracted from the images are actually polygons so we implemented the implicit, discrete curve shortening method found in [17]. As the curve evolves it is possible to end up with points along the curve that become very close. There is some research into adding a tangential component to the velocity to maintain an equal spacing of the points in the polygon [38]. Instead we calculated the average distance between consecutive points, and if two consecutive points are within one-fifth the average distance, we deleted one of the points. By the triangle inequality this cannot lengthen the curve. It is also possible for consecutive points to drift apart. We do not take any steps to correct this problem. The invariants were calculated using the formulas found by Boutin in [7].

4.2 Comparing signatures

An analytic regular planar curve is determined up to the action of the Euclidean group by its differential invariant signature. Although this tells us when two curves are exactly equal up to a group motion it is not clear how to use this information when two curves are perceptually close, but not exactly equivalent. We denote the space of signatures as $\mathcal{S}$. We want a function

$$\Phi : \mathcal{S} \times \mathcal{S} \to \mathbb{R}^+$$

such that Φ is larger if the curves related to the two signatures are perceptually close.

The signature of a curve will loop around a number of times in the (κ, κ_s) plane and will cross over the κ-axis at each vertex of the curve. To compare two signatures we break them down into a number of different segments, choosing each vertex as a place to break the signature and we call each portion of the signature a *signature segment*. We denote the space of signature segments as $\mathcal{S}'$.

4.2.1 Comparing segments

We use a set of features on the signature segments to compare them. We map each signature segment into $\mathbb{R}^3$ using the minimum and maximum of curvature as the first two coordinates and the length of the curve segment represented by the signature segment as the third coordinate. These features are relatively robust under different discretizations of the curve.

We compare the features using the function

$$\phi(x_i, y_j) = \sum_{k=1}^{3} w_k (x_i^k - y_j^k)^2 + \epsilon,$$

where w_i are weights chosen to normalize the different components and $\epsilon > 0$ is a small positive constant to ensure $\phi(x_i, y_j) > 0$. The range of values for the curvature is relatively much smaller than the range of values for the arc lengths

of the curves. To balance the different ranges of the components we set $w = (10000, 10000, 10)$. The other constant, ϵ, was chosen arbitrarily as $\epsilon = 10^{-5}$.

Now we have a way of comparing two different segments, but any given signature consists of an arbitrary number of segments, so we still need a way of comparing two arbitrary sized sets of signature segments. We create a resistor network with two sets of nodes, one for each signature segment in each signature. We make a complete bipartite graph between these sets of nodes, where the weight of the resistor connecting the i^{th} signature segment from the first signature to the j^{th} signature segment from the second signature is given by $\gamma_{i,j} = \phi(x_i, y_j)$. Each node in the first set is connected to a node of voltage +1 volts by a resistor of weight α_i and each node in the second set is connected to a node of voltage 0 volts by a resistor of weight β_j. We let $\alpha_i = m/2$ and $\beta_j = n/2$ where m is the number of segments in the first signature and n is the number of segments in the second signature. The values α_i, β_j were picked so that $0 < \Phi < 1$. We define $\Phi : \mathcal{S} \times \mathcal{S} \to \mathbb{R}^+$ as the total current that passes through this circuit. If many of the $\gamma_{i,j}$ are small, meaning many of the different segments match well, then Φ will be relatively large.

To calculate Φ we set up a linear system for the voltages of all the nodes of the circuit. Let A_i, B_j be the voltages on the nodes in the first and second set, respectively. Writing out Kirchhoff's laws we have

$$\frac{A_i - 1}{\alpha_i} + \sum_j \frac{A_i - B_j}{\gamma_{i,j}} = 0 \qquad \frac{-B_j}{\beta_j} + \sum_i \frac{A_i - B_j}{\gamma_{i,j}} = 0 \tag{4.1}$$

We can then solve for A_i, B_j because this is a diagonally dominant linear system for the voltages A_i, B_j. Let M be the matrix that is related to this linear system. The quantity $\sum_j \frac{B_j}{\beta_j}$ is the current passing through the circuit

$$M \begin{bmatrix} \vec{A}^T \\ \vec{B}^T \end{bmatrix} = \begin{bmatrix} \frac{\vec{1}}{\alpha} \\ \vec{0} \end{bmatrix}$$

$$\phi(X, Y) = \begin{bmatrix} \vec{0}^T & \frac{\vec{1}^T}{\beta} \end{bmatrix} M^{-1} \begin{bmatrix} \frac{\vec{1}}{\alpha} \\ \vec{0} \end{bmatrix}.$$

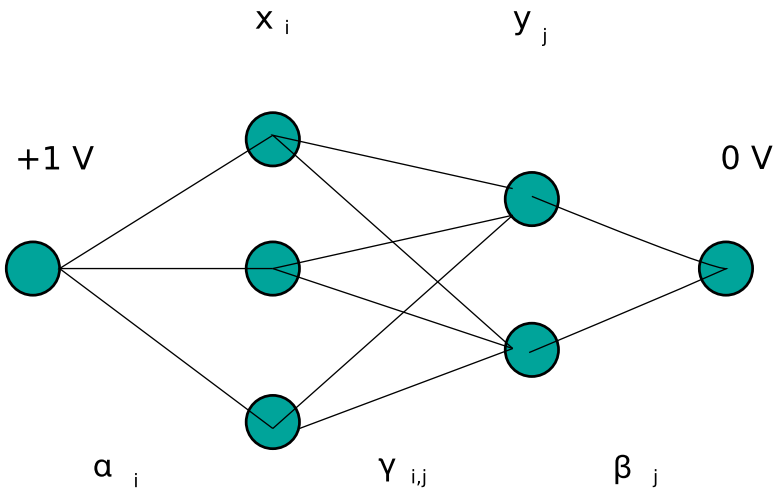

Figure 4.2: A diagram of a resistor network to compare 3 segments to 2 segments.

This method of comparing signatures should degrade well under occlusion. For example, we consider the case of comparing different segmentations of the palm tree. First we assume that the curves are smoothed enough so that the signatures match well. If we compare the curves from two complete segmentations, which include both the leaves and the trunk of the palm trees, then each signature segment from the first curve should have a closely matching signature segment in the second curve. This results in a large number of small resistors in our resistor network, and with many good paths the current through the circuit should be relatively large. If we one of the segmentations is partially occluded, for example if it is missing the trunk, then the rest of the curve should still match well. This would be similar to removing the nodes of the the circuit that corresponded to the trunk. The leaves of each curve still match well and the circuit still has a number of small resistors, so the current should still be relatively high.

4.3 Spectral clustering and machine learning

Now that we have a way of comparing any two curves, we can apply a wide variety of machine learning methods to the data. We first discuss spectral clustering. An overview of spectral clustering methods can be found at [55]. We describe the unnormalized graph Laplacian and how it can be used to create a mapping from the signatures to $\mathbb{R}^N$ which attempts to preserve the neighborhoods as represented by a similarity function. Normalized versions are discussed in [54],[44],[37].

We start with a dataset of M signatures $\{S_i\}$ where each signature has one of N different labels. We consider a completely connected graph (V, E) where each signature is a vertex and is connected to every other vertex by an edge of weight $A_{i,j} = \Phi(S_i, S_j)$. The *affinity matrix* A measures the similarity between any pair of signatures. The matrix

$$L = D - A,$$

where

$$D_{i,i} = \sum_j A_{i,j},$$

is known as the unnormalized graph Laplacian. The number of eigenvectors related to the eigenvalue 0 is exactly the number of connected components of the graph, and since our graph is connected it has multiplicity 1. We order the rest of the eigenvalues

$$0 = \lambda_0 < \lambda_1 \leq \lambda_2 \leq ... \leq \lambda_{M-1}$$

and consider the N eigenvectors $\mathbf{v}_1, \mathbf{v}_2, ..., \mathbf{v}_N$ corresponding to the eigenvalues $\lambda_1, \lambda_2, ..., \lambda_N$. Next we build the matrix $\mathbf{V}$ using $\mathbf{v}_1, \mathbf{v}_2, ..., \mathbf{v}_N$ as column vectors. We define $f(S_i)$ as the i^{th} row vector of $\mathbf{V}$, giving a mapping from our dataset into $\mathbb{R}^N$. Such spectral clustering methods attempt to preserve any neighborhoods in the data, so if $\Phi(S_i, S_j)$ is relatively large, then the points $f(S_i), f(S_j)$ should be relatively close together. This gives us a list of labeled points in $\mathbb{R}^N$ which is the starting point for many different machine learning methods, such as K-means or support vector machines. This process gives an embedding for all of our signatures

and can also be extended to new signatures as described by Bengio et.al. [6].

4.3.1 Training

Once we have a list of labeled data-points we train a binary classifier for each pair of labels. The binary classifiers were built using sparse multinomial logistic regression(SMLR) [32]. The final classifier was built by running all of the binary classifiers and choosing whichever class received the most votes out of all of the classifiers. For the most part, it did not seem that changing the binary classifier made much of a difference in the performance of the classifiers.

4.3.2 Leave-one-out cross-validation

To estimate the error rate of our classifier we use leave-one-out cross-validation, a standard machine learning cross-validation technique. In leave-one-out cross-validation we leave out one element from the dataset for validation and train our classifier using the rest of the dataset. We run the classifier on the validation element and check to see if it has returned the correct label. We estimate the error rate η of the classifier by rotating the validation element through the entire dataset

$$\eta = \frac{\#\text{ Errors}}{\#\text{ of total Signatures}}.$$

4.3.3 Stopping time

Most of the curves start out very noisy. If we look at the signatures of the unsmoothed curves, they all appear to be the same, they are taking into account very local features which are noise. They do not capture the common features of the curves of the same label, which would let us learn these labels. As the curves flow under the curve shortening flow they begin to look like the other curves of the same label. However, the area decreases at a constant rate, so the curve shortening flow only exists for a finite period of time. Even before the curves disappear they

will all begin to look like small circles before they disappear. If the curves are smoothed too much all the differences between the different labels will disappear. Somewhere in between should be a happy medium where the different classes are separated from each other, but before the differences between the different classes have disappeared. We smooth the entire database of curves for a number of steps and rerun the training and cross-validation after each time-step to check the error rate. After smoothing through a number of steps we take the time-step with the lowest error rate. We call this stopping time $\hat{t}$. To extend this method to a new curve, we would smooth it for this amount and compare it to an equally smoothed version of all the curves in the database. Looking at the error rates we see that it seems to generally flatten out over a fairly wide range of time steps.

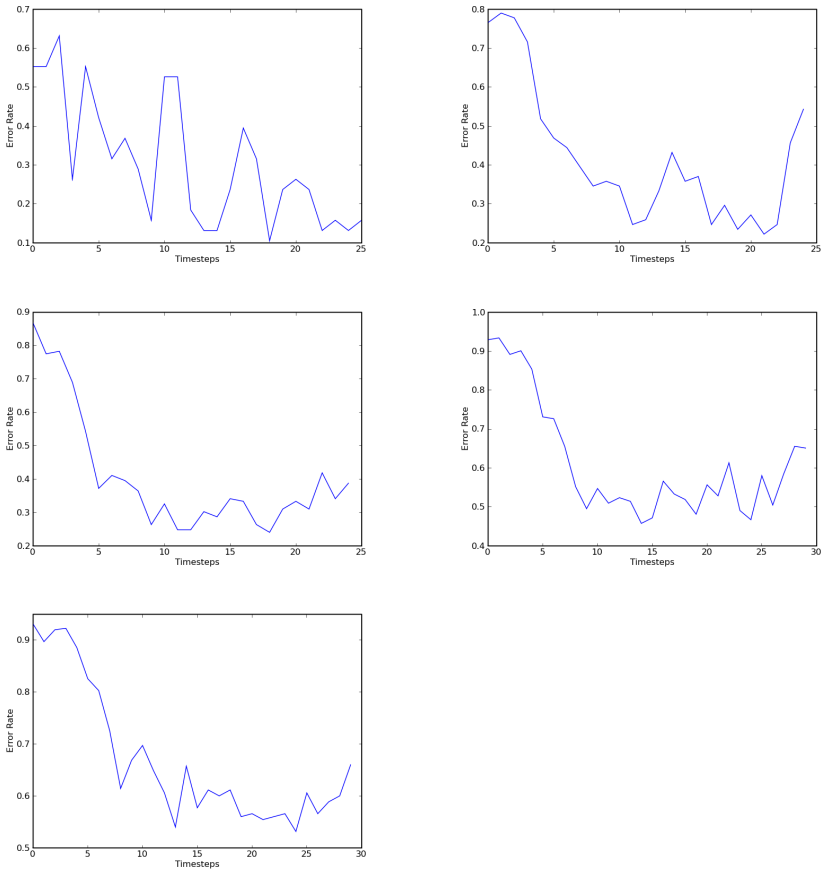

Figure 4.3: Error rate of SMLR classifier at each different scale for a number of different classes

4.4 Shape search

We can also use the tools that we have built to create a database of objects, which we can search by shape. Since we have a function to compare any two curves we consider a nearest-neighbor method, where we find labels by looking at the labels of closely matching curves. We consider each curve as a query that returns a list of k labels, and we consider the search a success if the correct label of the query is found amongst these k labels. To decide which labels to return we first smooth all of the curves. The amount of smoothing depends on the total number of different labels we are including in our experiment and is chosen as described in section 4.3.3. Once the curves have been smoothed we compare the query curve to all of the other curves using our function Φ. To find the closest matching curves we then sort by the values return by Φ. We return the labels of the top matching curves, until we have returned k different labels. Since each label has at least 5 different curves this process will most likely return more then k curves. We repeat this experiment a number of times including a different number of labels and for different values of k. The recall rate given in the tables below is found by taking the number of successful searches and dividing by the total number of curves.

Looking at the results in the tables below we find the correct label amongst the top two over 94% of the time, except for the experiment with 20 labels. The stopping time for our experiment with 20 labels is smaller. Perhaps a larger smoothing time would lead to better results.

8 labels	$\hat{t} = 21$
k	Recall
1	0.90
2	0.95
3	0.96
4	0.98
5	1

12 labels	$\hat{t} = 18$
k	Recall
1	0.90
2	0.97
3	0.98
4	1

20 labels	$\hat{t} = 14$
k	Recall
1	0.79
2	0.86
3	0.93
4	0.94
5	0.95
6	0.96
7	0.97
8	0.98
9	0.99
10	1.00

33 labels	$\hat{t} = 24$
k	Recall
1	0.87
2	0.94
3	0.95
4	0.97
5	0.97
6	0.97
7	0.97
8	0.98
9	0.98
10	0.98

Chapter 5

Conclusion

In this thesis we have given an overview of Cartan's method of normalization, and Olver's work on regularized group actions which leads to the invariant variational complex. We include calculations of the Euler and Hamilton operators for the Euclidean group, equi-affine group and the similarity group acting on planar curves, and the centro-affine group acting on curves in $\mathbb{R}^3$. The Euler operators allow us to compute the evolution of differential invariant signatures for various invariant curve flows. Under the curve shortening flow we reprove some results such as Angenent's result on the non-increase of the number of vertices, the evolution of global geometric quantities, such as the arc length, and find some particular invariant solutions such as the grim-reaper curves. The no new vertex theorem can be extended for specific flows that are invariant under the equi-affine group and the similarity group. In the case of the centro-affine group acting on space curves we find a signature that corresponds to a time-invariant flow.

Along with the study of the evolution of the differential invariant signatures we also include the results of a study using invariant signatures and the curve shortening flow to recognize curves. The curves, which were extracted as the boundaries of human segmented regions in images, vary in the small details. These small differences are usually problems for differential invariants since they are sensitive to noise. We show that these differences largely seem to disappear when the curves

are smoothed with the curve shortening flow. Using a simple method of comparing signatures and the right amount of smoothing, we can usually determine the correct label for any particular curve in our database.

There is still work to be done on both sides of this problem. On the pure side, invariant curve flows often lead to integrable soliton dynamics, but the connection between the two has not been well studied. While we have provided a relatively simple idea for comparing signatures, it is possible that a method using more information from the signature or from multiple scales would be able to perform better at classifying the curves. The curve shortening flow is well studied, has a number of nice properties, and has been widely recommended as a tool for shape modelling, but, ideally we would like to show some connection between the evolution that we apply to the curves and to the method we use to compare them. It would also be interesting to see these methods extended to other group actions or to recognizing surfaces.

Chapter 6

Bibliography

References

[1] M. Abramowitz and I. Stegun. *Handbook of Mathematical Functions*. Dover, 1972.

[2] I. M. Anderson. The variational bicomplex, Utah State technical report, 1989.

[3] S. Angenent. Parabolic equations for curves on surfaces I: Curves with p-integrable curvature. *Ann. of Math*, 132(2):451–483, 1990.

[4] S. Angenent. Parabolic equations for curves on surfaces II: Intersections, blow-up and generalized solutions. *Ann. of Math*, 133(2):171–215, 1991.

[5] S. Angenent, G. Sapiro, and A. Tannenbaum. On the affine heat equation for nonconvex curves. *J. Amer. Math. Soc*, 11:601–634, 1994.

[6] Y. Bengio, J.-F. Paiement, P. Vincent, O. Delalleau, N. L. Roux, and M. Ouimet. Out-of-sample extensions for LLE, Isomap, MDS, Eigenmaps, and spectral clustering. In *Advances in Neural Information Processing Systems*, volume 17, pages 177–184. MIT Press, 2004.

[7] M. Boutin. Polygon regognition and symmetry detection. *Foundations of Computational Mathematics*, 3:227–271, 2003.

[8] P. Broadbridge and P. Tritscher. An integrable fourth-order nonlinear evolution equation applied to thermal grooving of metal surfaces. *IMA J. Appl. Math.*, 53:249–265, 1994.

[9] A. Bruckstein, G. Sapiro, and D. Shaked. Evolutions of planar polygons. *International Journal of Pattern Recognition and Artificial Intelligence*, 10:991–1014, 1995.

[10] J. Cahn, C. Elliot, and A. Novick-Cohen. The Cahn-Hilliard equation with a concentration dependent mobility: Motion by minus the Laplacian of the mean curvature. *European Jounral Applied Mathematics*, 7:287–301, 1996.

[11] J. Cahn and J. Taylor. Surface motion by surface difusion. *Acta Metallurgica*, 42:1045–1063, 1994.

[12] E. Calabi, P. J. Olver, C. Shakiban, A. Tannenbaum, and S. Haker. Differential and numerically invariant signature curves applied to object recognition. *Int. J. Computer Vision*, 26:107–135, 1998.

[13] E. Calabi, P. J. Olver, and A. Tannenbaum. Affine geometry, curve flows, and invariant numerical approximations. *Adv. in Math*, 124:154–196, 1996.

[14] E. Cartan. La méthode du repère mobile, le théorie des groupes continus, et les espaces généralisés. *Exposés de Géométrie*, 5, 1935.

[15] E. Cartan. A théorie des groupes finis et continus et la géométrie différentielle traitées par la méthode du reprére mobile. *Cahiers Scientifiques*, 18, 1937.

[16] K.-S. Chou and X.-P. Zhu. *The Curve Shortening Problem*. CRC/Chapman and Hall, 2001.

[17] K. Deckelnick, G. Dziuk, and C. Elliot. Computation of geometric partial differential equations and mean curvature flow. *Acta Numerica*, pages 139–232, 2005.

[18] M. Desbrun, M. Meyer, P. Schröder, and A. H. Barr. Implicit fairing of irregular meshes using diffusion and curvature flow. In *SIGGRAPH '99:*

Proceedings of the 26th annual conference on computer graphics and interactive techniques, volume 26, pages 317–324, New York, NY, USA, 1999. ACM Press/Addison-Wesley Publishing Co.

[19] C. Ehresmann. Introduction à la thèorie des structures infinitèsimales et des psueod-groupes di Lie. *Gómetri Différentielle*, 1953.

[20] J. Escher and G. Simonett. The volume preserving mean curvature flow near spheres. *Proc. Amer. Math. Soc.*, 126(9):2789–2796, 1998.

[21] M. Fels and P. J. Olver. Moving coframes – I. A practical algorithm. *Acta Appl. Math.*, 51:161–213, 1997.

[22] M. Fels and P. J. Olver. Moving coframes – II. Regularization and theoretical foundations. *Acta Appl. Math.*, 55:127–208, 1999.

[23] M. Gage. On an area-preserving evolution equation for plane curves. *Contemporary Mathematics*, pages 51–62, 1986.

[24] M. Gage and R. S. Hamilton. The heat equation shrinking convex plane curves. *J. Differential Geom.*, 23(1):69–96, 1986.

[25] Y. Giga and K. Ito. Loss of convexity of simple closed curves moved by surface diffusion, topics in nonlinear analysis. *Progr. Nonlinear Differential Equations Appl.*, 35:305–320, 1999.

[26] M. Grayson. The heat equation shrinks embedded plane curves to round points. *J. Differential Geom.*, 26(2):285–314, 1987.

[27] M. Hanke, Y. O. Halchenko, P. B. Sederberg, S. J. Hanson, J. V. Haxby, and S. Pollmann. PyMVPA: A Python toolbox for multivariate pattern analysis of fMRI data. *Neuroinformatics*, 2009.

[28] G. Huisken. The volume preserving mean curvature flow. *J. Reine. Angew. Math.*, pages 35–48, 1987.

[29] M. Kass, A. Witkin, and D. Terzopoulos. Snakes: Active contour model. *International Journal of Computer Vision*, 1:321–331, 1988.

[30] I. A. Kogan. Inductive construction of moving frames. *Contemporary Mathematics*, 285:157–170, 2001.

[31] I. A. Kogan and P. J. Olver. Invariant Euler-Lagrange equations and the invariant variational bicomplex. *Acta Appl. Math*, 76:137–193, 2000.

[32] B. Krishnapuram, M. Figueiredo, L. Carin, and A. Hartemink. Sparse multinomials logistic regression: Fast algorithims and generalization bounds. *IEEE Transactions on Pattern Analysis and Machine Intelligence (PAMI)*, 27:957–968, 2005.

[33] S. Loncaric. A survey of shape analysis techniques. *Pattern Recognition*, 31(8):983–1001, 1998.

[34] R. Malladi, J. A. Sethian, and B. C. Vemuri. Shape modeling with front propagation: A level set approach. *IEEE Transactions on Pattern Analysis and Machine Intelligence*, 17:158–175, 1995.

[35] D. Martin, C. Fowlkes, D. Tal, and J. Malik. A database of human segmented natural images and its application to evaluating segmentation algorithms and measuring ecological statistics. *Proc. 8th Int'l Conf. Computer Vision*, 2:416–423, July 2001.

[36] U. F. Mayer. A singular example for the averaged mean curvature flow. *Experiment. Math.*, 10:103–107, 2001.

[37] M. Meila and J. Shi. A random walks view of spectral segmentation. *AISTATS*, 2001.

[38] K. Mikula and D. Sevcovic. Computational and qualitative aspects of evolution of curves driven by curvature and external force. *Computing and Visualization in Science*, 6:211–225(15), April 2004.

[39] F. Mohktarian and M. Bober. *Curvature Scale Space Representation: Theory, Applications, and MPEG-7 Standardization.* Computational Imaging and Vision. Springer, 2003.

[40] F. Mokhtarian. Silhoutte based isolated object recognition through curvature scale space. *IEEE Transactions on Pattern Analysis and Machine Intelligence*, 17(5):539 – 544, 1995.

[41] F. Mokhtarian and A. Mackworth. A theory of multiscale, curvature-based shape representation for planar curves. *IEEE Transactions on Pattern Analysis and Machine Intelligence*, 14(8):789–805, 1992.

[42] S. Mukhopadhyaya. New methods in the geometry of a plane arc. *Bulletin Calcutta Mathematics Society*, 1:31–37, 1909.

[43] E. Musso and L. Nicoldi. Invariant signatures of closed planar curves. *Journal of Mathematical Imaging and Vision*, 35:68–85, 2009.

[44] A. Y. Ng, M. I. Jordan, and Y. Weiss. On spectral clustering: Analysis and an algorithm. *Advances in Neural Information Processing Systems*, 14:849–856, 2001.

[45] P. Olver. Moving frames and joint differential invariants. *Regular and Chaotic Dynamics*, 4:3–18, 1999.

[46] P. Olver. Moving frames and singularites of prolonged group actions. *Selecta Math*, 6:41–77, 2000.

[47] P. Olver, G. Sapiro, and A. Tannenbaum. Differential invariant signatures and flows in computer vision: A symmetry group approach. In *Geometry-Driven Diffusion in Computer Vision.* Kluwer Academic Publishers, 1994.

[48] P. Olver, G. Sapiro, and A. Tannenbaum. Invariant geometric evolutions of surfaces and volumetric smoothing. *SIAM J. Appl. Math.*, 57:176–19, 1997.

[49] P. J. Olver. *Equivalence,Invariants, and Symmetry*. Cambridge University Press, Cambridge, UK, 1995.

[50] P. J. Olver. Moving frames. *J. Symb. Comput.*, 36(3-4):501–512, 2003.

[51] P. J. Olver. Invariant submanifold flows. *Journal of Physics A: Mathematical and Theoretical*, 41(34), 2008.

[52] L. Ovsiannikov. *Group Analysis of Differential Equations*. Academic Press, New York, 1982.

[53] G. Sapiro and A. Tannenbaum. Area and length preserving geometric invariant scale-spaces. *IEEE Transactions on Pattern Analysis and Machine Intelligence*, 17(1):67–72, 1995.

[54] J. Shi and J. Malik. Normalized cuts and image segmentation. *IEEE Transactions on Pattern Analysis and Machine Intelligence*, 22:888–905, 2000.

[55] U. von Luxburg. A tutorial on spectral clustering. *Statistics and Computing*, 17:395–416, 4 2007.